

University of Windsor

Scholarship at UWindor

Electronic Theses and Dissertations

Theses, Dissertations, and Major Papers

2010

Modeling and Control of a Proton Exchange Membrane Fuel Cell-Battery Power System

Yan Zngang

University of Windsor

Follow this and additional works at: <https://scholar.uwindsor.ca/etd>

Recommended Citation

Zngang, Yan, "Modeling and Control of a Proton Exchange Membrane Fuel Cell-Battery Power System" (2010). *Electronic Theses and Dissertations*. 8057.

<https://scholar.uwindsor.ca/etd/8057>

This online database contains the full-text of PhD dissertations and Masters' theses of University of Windsor students from 1954 forward. These documents are made available for personal study and research purposes only, in accordance with the Canadian Copyright Act and the Creative Commons license—CC BY-NC-ND (Attribution, Non-Commercial, No Derivative Works). Under this license, works must always be attributed to the copyright holder (original author), cannot be used for any commercial purposes, and may not be altered. Any other use would require the permission of the copyright holder. Students may inquire about withdrawing their dissertation and/or thesis from this database. For additional inquiries, please contact the repository administrator via email (scholarship@uwindsor.ca) or by telephone at 519-253-3000ext. 3208.

Modeling and Control of a Proton Exchange Membrane Fuel Cell-Battery Power System

by

Yan Zhang

**A Thesis
Submitted to the Faculty of Graduate Studies
through Mechanical, Automotive, and Materials Engineering
in Partial Fulfillment of the Requirements for
the Degree of Master of Applied Science at the
University of Windsor**

Windsor, Ontario, Canada

2010

© 2010 Yan Zhang



Library and Archives
Canada

Published Heritage
Branch

395 Wellington Street
Ottawa ON K1A 0N4
Canada

Bibliothèque et
Archives Canada

Direction du
Patrimoine de l'édition

395, rue Wellington
Ottawa ON K1A 0N4
Canada

Your file Votre référence

ISBN: 978-0-494-90380-3

Our file Notre référence

ISBN: 978-0-494-90380-3

NOTICE:

The author has granted a non-exclusive license allowing Library and Archives Canada to reproduce, publish, archive, preserve, conserve, communicate to the public by telecommunication or on the Internet, loan, distribute and sell theses worldwide, for commercial or non-commercial purposes, in microform, paper, electronic and/or any other formats.

The author retains copyright ownership and moral rights in this thesis. Neither the thesis nor substantial extracts from it may be printed or otherwise reproduced without the author's permission.

AVIS:

L'auteur a accordé une licence non exclusive permettant à la Bibliothèque et Archives Canada de reproduire, publier, archiver, sauvegarder, conserver, transmettre au public par télécommunication ou par l'Internet, prêter, distribuer et vendre des thèses partout dans le monde, à des fins commerciales ou autres, sur support microforme, papier, électronique et/ou autres formats.

L'auteur conserve la propriété du droit d'auteur et des droits moraux qui protègent cette thèse. Ni la thèse ni des extraits substantiels de celle-ci ne doivent être imprimés ou autrement reproduits sans son autorisation.

In compliance with the Canadian Privacy Act some supporting forms may have been removed from this thesis.

While these forms may be included in the document page count, their removal does not represent any loss of content from the thesis.

Conformément à la loi canadienne sur la protection de la vie privée, quelques formulaires secondaires ont été enlevés de cette thèse.

Bien que ces formulaires aient inclus dans la pagination, il n'y aura aucun contenu manquant.

Canada

ABSTRACT

A general methodology of modeling, control and building a proton exchange membrane fuel cell-battery system is introduced in this thesis. A set of fuel cell-battery power system model has been developed and implemented into Simulink environment. The model is able to address the dynamic behaviours of PEM fuel cell stack, boost DC/DC converter and lithium-ion battery. In order to control the power system to achieve a proper performance, a set of system controller including a PEM fuel cell reactant supply control, a humidification controller, and a power management controller was developed based on the system model.

A physical 100W PEM fuel cell-battery power system using microcontroller as embedded controller is built to validate the simulation results as well as demonstrate this new environment-friendly power source. Experimental results show that the 100W PEM fuel cell-battery power system can operate automatically with the varying load condition as a stable power supply. The experiment results follow the basic trend of the simulation results.

DEDICATION

To my parents

ACKNOWLEDGEMENTS

First, I would like to give my most sincere gratitude to my advisor, Dr. Biao Zhou, for his patient guidance and selfless support during the past two years. I appreciate the opportunity and the challenge he gave me to work under his supervision in his group. I could not have finished the Master's level study without the knowledge, encouragement, and the positive attitude from him. This study and thesis could not have been possible without him.

Also, I would like to thank Dr. Shaohong Cheng, Dr. David Ting, and Dr. Xueyuan Nie for the time and efforts they put on the proposal and defense of my thesis.

My appreciation also goes to my great team mates: Le Dinh Anh, Jonnalagedda Srikanth, Xiaojing Liu, Ahmad Fadel, Dan Denomme , Boutros Charbel, Nguyen Anh Tuan, Simo Kang, Season Wang, Zhi Shang, Rui Hu, Esi Navaei Alvar. Those hardworking day and night and joyful moments with them will always in my memory.

Finally, I would like to give many thanks to my parents. It is their spiritual, emotional and mental support which helps me through every hard time.

TABLE OF CONTENTS

ABSTRACT	III
DEDICATION.....	IV
ACKNOWLEDGEMENTS.....	V
LIST OF FIGURES	IX
1. INTRODUCTION.....	1
1.1 Fuel cell.....	1
1.2 PEM fuel cell.....	3
1.3 PEM fuel cell system	6
1.3.1 Stream flow control subsystem	6
1.3.2 Water management subsystem.....	8
1.3.3 Thermal management subsystem	9
1.4 PEM fuel cell-battery power system	9
1.4.1 Power management subsystem	10
1.5 Literature review	10
1.5.1 PEM fuel cell system modeling and control	10
1.5.2 PEM fuel cell-battery power system.....	11
1.6 Motivation.....	12
1.7 Objective	13
1.8 Thesis overview	14
2. PEM FUEL CELL STACK MODEL	15
2.1 PEM fuel cell flow dynamics.....	15

2.1.1 Mass flow governing equations	16
2.1.2 Stack pressure change	17
2.1.3 Relative humidity inside stack	19
2.1.4 Water transfer across membrane	19
2.2 Electrochemical model.....	21
2.3 Air and hydrogen supply model.....	23
3. FUEL CELL-BATTERY POWER SYSTEM AUXILIARY MODEL.....	24
3.1 Air blower model	24
3.2 DC/DC converter model	26
3.3 Battery model.....	27
3.4 Humidifier model.....	29
4. PEM FUEL CELL-BATTERY POWER SYSTEM CONTROLS.....	32
4.1 PEM fuel cell stack flow control.....	32
4.1.1 Air supply control	32
4.1.2 Hydrogen flow control	33
4.1.3 Simulation of PEM fuel cell stack system	34
4.2 Humidification control	38
4.2.1 Liquid water control.....	39
4.2.2 Feedback controller for humidifier	40
4.2.3 Simulation results of humidifier control	40
4.3 Parametric Study of PEM fuel cell stack system	43
4.3.1 Temperature effect	44
4.3.2 Relative humidity effect.....	45

4.3.3 Cathode inlet pressure effect	47
4.3.4 Oxygen excess ratio effect	48
4.4 Power management of PEM fuel cell-battery power system	49
4.4.1 Simulation conditions.....	50
4.4.2 Results and discussion.....	50
5. PORTABLE PEM FUEL CELL-BATTERY SYSTEM WITH EMBEDDED CONTROL SYSTEM.....	56
5.1 System explained	56
5.2 Experimental Study on simulation results validation and Portable PEM fuel cell-battery system performance	57
5.2.1 validation of PEM fuel cell control system simulation.....	57
5.2.2 Portable pem fuel cell-battery power system performance.....	60
6. CONCLUSIONS AND RECOMMENDATIONS.....	63
6.1 Conclusions	63
6.2 Recommendations	63
REFERENCES.....	65
VITA AUCTORIS.....	69

LIST OF FIGURES

FIGURE 1. A SIMPLE FUEL CELL OPERATION[1].....	2
FIGURE 2. PEM FUEL CELL OPERATION	4
FIGURE 3. BOOST DC/DC CONVERTER	26
FIGURE 4. ON-OFF STATE EXPLAINED OF BOOST DC/DC CONVERTER	26
FIGURE 5. FEED FORWARD CONTROL ALGORITHM FOR PEM FUEL CELL AIR SUPPLY CONTROL	33
FIGURE 6. FEED FORWARD CONTROL ALGORITHM FOR PEM FUEL CELL HYDROGEN SUPPLY CONTROL	33
FIGURE 7. PEM FUEL CELL POLARIZATION CHARACTERISTIC	34
FIGURE 8. SERIAL STEP LOAD INPUT	35
FIGURE 9. VOLTAGE RESPONSE TO STEP INPUT.....	36
FIGURE 10. OUTPUT VOLTAGE TRANSIENT WHEN INPUT CURRENT CHANGE FROM 100A TO 130A	36
FIGURE 11. PEM FUEL CELL OUTPUT POWER RESPONSE	37
FIGURE 12. RELATIVE HUMIDITY CHANGE DUE TO STEP CURRENT INPUT.....	38
FIGURE 13. HUMIDIFICATION CONTROLLER BLOCK DIAGRAM	40
FIGURE 14. POLARIZATION CURVE WITH AND WITHOUT HUMIDIFIER CONTROL	40
FIGURE 15. OUTPUT VOLTAGES WITH AND WITHOUT HUMIDIFIER CONTROL.....	41
FIGURE 16. OUTPUT POWERS WITH AND WITHOUT HUMIDIFIER CONTROL.....	41
FIGURE 17. RELATIVE HUMIDITY WITH AND WITHOUT HUMIDIFIER CONTROL.....	42
FIGURE 18. MEMBRANE WATER CONTENT WITH AND WITHOUT HUMIDIFIER CONTROL.....	43
FIGURE 19. STEP SIGNAL INPUT FOR PARAMETRIC STUDY	44

FIGURE 20. FUEL CELL VOLTAGE RESPONSE IN DIFFERENT STACK TEMPERATURE	44
FIGURE 21. FUEL CELL POWER RESPONSE IN DIFFERENT TEMPERATURE	45
FIGURE 22. FUEL CELL OUTPUT VOLTAGE IN DIFFERENT MEMBRANE WATER CONTENT	45
FIGURE 23. FUEL CELL POWER RESPONSE IN DIFFERENT MEMBRANE WATER CONTENT	46
FIGURE 24. FUEL CELL VOLTAGE RESPONSE IN DIFFERENT CATHODE INLET PRESSURE	47
FIGURE 25. FUEL CELL POWER RESPONSE IN DIFFERENT CATHODE INLET PRESSURE	47
FIGURE 26. FUEL CELL VOLTAGE RESPONSE IN DIFFERENT OXYGEN EXCESS RATIO	48
FIGURE 27. FUEL CELL POWER RESPONSE IN DIFFERENT OXYGEN EXCESS RATIO	48
FIGURE 28. LOAD-REQUIRED POWER	51
FIGURE 29. REQUIRED FUEL CELL CURRENT	52
FIGURE 30. FUEL CELL PRODUCED POWER AND VOLTAGE	53
FIGURE 31. REGULATED FUEL CELL POWER AND VOLTAGE	53
FIGURE 32. BATTERY POWER	53
FIGURE 33. BATTERY SOC	54
FIGURE 34. AUXILIARY-CONSUMED POWER	54
FIGURE 35. LOAD-REQUIRED POWER VS. SYSTEM PRODUCED POWER	54
FIGURE 36. PORTABLE PEM FUEL CELL-BATTERY POWER SYSTEM DIAGRAM	56
FIGURE 37. STEP CURRENT INPUT FOR SIMULATION AND EXPERIMENT	57
FIGURE 38. VOLTAGE OUTPUT FOR SIMULATION AND EXPERIMENT	58
FIGURE 39. POWER OUTPUT FOR SIMULATION AND EXPERIMENT	59
FIGURE 40. STEP CURRENT DEMAND INPUT	60
FIGURE 41. SYSTEM VOLTAGE OUTPUT	61
FIGURE 42. SYSTEM POWER OUTPUT	62

1. INTRODUCTION

1.1 FUEL CELL

To reduce greenhouse emissions, the demand of an environment-friendly energy source has greatly increased during the past decades. Fuel cells, as one of the promising new generation power sources, are widely used in both automotive and stationary applications now a days, due to their high power density, high efficiency and low emission.

Fuel cells are electrochemical devices which convert chemical energy from fuels into electricity. Not like the conventional battery, a sealed energy storage device, fuel cell is more like an energy factory, as long as fuel is supplied, it will continually generate electricity [1]. A fuel cell is usually formed by two electrodes, called anode and cathode, which are separated by an electrolyte. The electrolyte is made of special material which can be passed through by protons but not electrons.

The first fuel cell was invented by William R. Grove in 1839. Figure 1 [1] explains the basic operation of a simple H_2-O_2 fuel cell. This fuel cell uses two platinum electrodes and dips them into an aqueous acid electrolyte. Hydrogen gas supplied to the left electrode (anode) is split into protons (H^+) and electrons. The protons can go through the electrolyte, but the electrons are blocked. Instead, the electrons flow are forced to go through the external wire that connects the two platinum electrodes from left to right a piece of wire that connects the two platinum electrodes, thus, electricity is created.

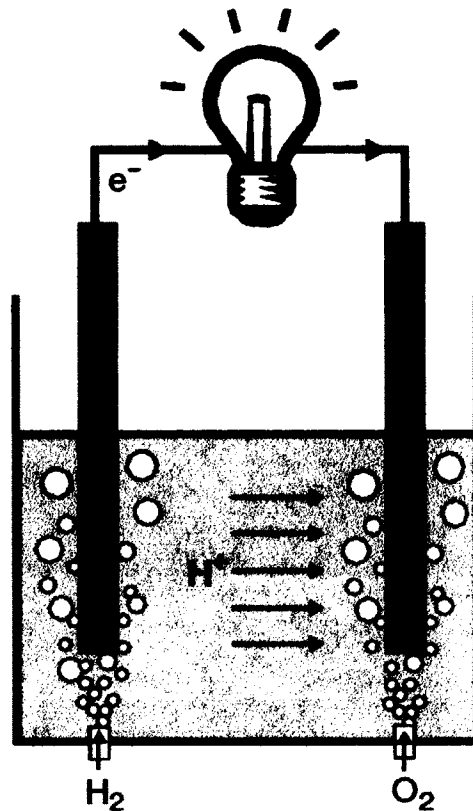


Figure 1. A Simple fuel cell operation[1]

The fuel cell converts chemical energy from fuel directly into electricity by electro-chemical reaction, so the fuel cell reaction is not limited by Carnot Cycle Limitation. That is why the maximum efficiency of fuel cell is considered much higher than conventional internal combustion engine.

Many different types and sizes of fuel cells are invented in the search for greater efficiency. Usually the types of fuel cells are classified by different electrolyte. Today, there are five major types of fuel cell, as shown in table 1: alkali, molten carbonate,

phosphoric acid, proton exchange membrane (PEM) and solid oxide. The first three are liquid electrolytes; the last two are solids.

Table 1. Different types of fuel cells

Type	Efficiency	Operation Temperature	Use
Polymer Electrolyte Membrane Fuel Cell (PEMFC)	50%	80° C	Transportation – cars, buses, boats, trains, scooters, bikes Residential – household electrical power needs Portable – laptop computers, cell phones, medical equipment
Alkali Fuel Cell (AFC)	60%	100-220° C	NASA space program – space vehicles
Phosphoric Acid Fuel Cell (PAFC)	40%	200° C	Landfill/wastewater treatment facilities – To generate power from methane gas
Solid Oxide Fuel Cell (SOFC)	55%	600-1000° C	Commercial-utility power plants, airport terminals schools, office building, hotels, hospitals.
Molten Carbonate Fuel Cell (MCFC)	55%	650° C	Commercial-utility power plants, airport terminals, schools, office building, hotels, hospitals

Among these fuel cells Proton Exchange Membrane fuel cell generate more power for a given volume or weight of fuel cell And it operates in low temperature, has a solid electrolyte, is suitable for stationary and portable power source application. Thus, PEM fuel cell is selected as research object in this study.

1.2 PEM FUEL CELL

Polymer electrolyte membrane fuel cell (PEMFC), also been called proton exchange membrane fuel cells, uses thin polymer sheets coated with a thin layer of platinum catalyst as an electrolyte. The catalyst is used to increase the speed of reaction; otherwise

the reaction will only happen in high temperature. Its electrodes are made of porous carbon.

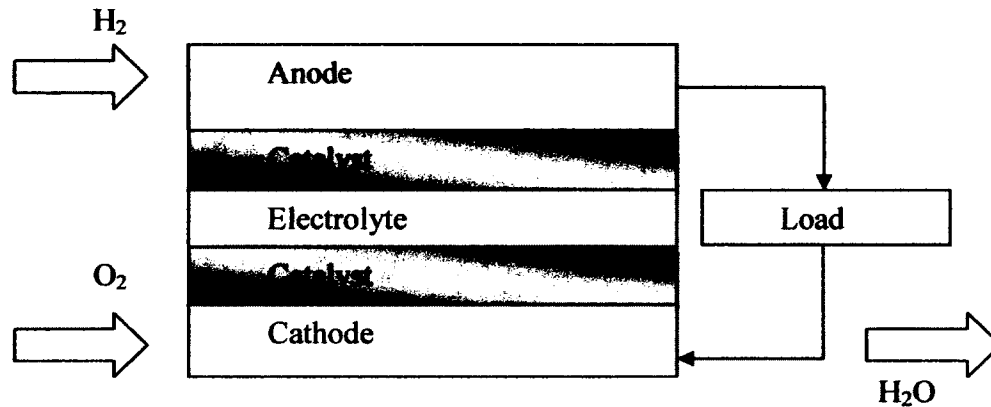


Figure 2. PEM fuel cell operation

Figure 2 explains the operation of the PEM fuel cell. When hydrogen is supplied to the anode, it will go through anode channel and reach the catalyst later. The hydrogen molecular will separate into hydrogen will be ionized into H⁺ ions and electrons. The hydrogen ions will pass the membrane to cathode side but the electrons cannot go through membrane due to its electron-insulate property. The electrons must go through the external circuit to reach the cathode side and meet the ions, thus, the electricity is produced. In the cathode side, the supplied oxygen will react with hydrogen ions and electrons to produce water and small amount of heat. The whole electrochemical reaction can be addressed by the following equations:



Usually the single PEM fuel cell output voltage is varying between 0.6-1 volts, and it highly depends on the operating conditions like temperature, humidity, reactants pressure, etc. In order to achieve high output voltage and power, people place each single cell in serial and connect them with conducting bridges so that a stack is formed. The output voltage of a stack is the total of each single cell.

PEM fuel cell was invented by General Electric in the early 1960s. It was used as part of the National Aeronautic Space Administration (NASA) program in the beginning of the U.S. Gemini space program. Most major automakers today are developing their PEM fuel cells cars to achieve the more and more tighten regulations of lower emission and energy consumption. The PEM fuel cells powered houses have been testing since 1998 and demonstration units are now available.

PEM fuel cell is about 40 to 50 percent efficient. If it is used with cogenerate equipment, the efficiency could be increased to about 80 percent. PEM fuel cells operate at low temperatures (about 80° C), which makes them suitable for use in portable devices, cars, and houses. Very little warm-up time is required, and PEM fuel cells respond immediately to increased demand for power. Since water is the only liquid in this fuel cell, it can be considered 'zero emission' power source.

Other then these advantages of PEM fuel cell, there are still some drawbacks prevent PEM fuel cell technology to be commercialized. The platinum used to coat the electrolyte is expensive; and after less than two years of operation, the electrolyte must

typically be replaced. The electrolyte must be well humidified during the whole operation to keep its performance; and the hydrogen must be very pure. The need to increase life and decrease cost is the main barriers to widespread use of PEM fuel cells.

1.3 PEM FUEL CELL SYSTEM

As explained in table 1.1, PEM fuel cell stack can be used in many applications from automotive industry to portable power devices. But PEM fuel cell stack cannot operate individually to generate electricity. It has to be integrated with many auxiliaries to form a system in order to produce electric energy.

1.3.1 STREAM FLOW CONTROL SUBSYSTEM

Fuel cell has to be supplied with reactants continually in order to produce electricity. So stream flow control subsystem is the most important subsystem in fuel cell system. This subsystem consists of two parts, fuel supply subsystem and air supply subsystem. The goal of reactants supply subsystem is to provide sufficient reactants to fuel cell stack, preventing stack starvation and affecting fuel cell system performance.

In PEM fuel cell, only pure hydrogen gas can be used as fuel. To supply pure hydrogen gas to PEM fuel cell, two ways are possible to achieve the goal. The first one is to use a fuel reformer to convert conventional fuel such as natural gas or methane into pure hydrogen gas. The procedure is to use a fuel pump to pump the conventional fuel into the fuel reformer and pure hydrogen will come out of fuel reformer and supplied to PEM fuel cell. The hydrogen flow rate can be controlled by varying the pressure of the

fuel pump. The fuel reforming methods has their advantages of fuel flexibility; also, pure hydrogen gas is not a very energy dense fuel, the energy it contents is very little compared to liquid fuel like methanol or gasoline. So choose the low cost fuel to supply the fuel cell system could significantly reduce the daily cost in energy consumption. On the other hand, the fuel reformer itself is also a energy consume device. It will increase the fuel cell system auxiliary power consumption. Usually when the fuel cell system is used on a vehicle or a building, the system will produce a large amount of electricity from several kilowatts to thousands kilowatts, so the energy consumed by system auxiliaries can be ignored. But when the fuel cell system is used on very small or portable application, the auxiliaries consumed energy must be kept as low as possible. The other way to supply hydrogen is to directly supply hydrogen from a high pressure tank, use control valve or mass flow controller to control the hydrogen flow rate. This method could reduce the energy consumed by fuel reformer and is suitable for small fuel cell system application. We will use high pressure hydrogen tank as hydrogen source in this study.

In cathode side of PEM fuel cell, air is usually used instead of pure oxygen. The main components in air are oxygen, nitrogen and water vapor. So using air instead of pure oxygen could reduce system operating cost and in the same time water vapor could be used to humidify the fuel cell membrane. The air is supplied into cathode by blower fan or motor-driven compressor. Cathode inlet pressure has great effect on fuel cell performance, so keep high inlet pressure is a major task for air supply system. On the other hand, getting high output voltage from blower or compressor will require high

power consumption by motor. So doing the trade off between getting high cathode inlet pressure and keep minimal power consumption by blower motor is critical for cathode flow control.

Purging control in both cathode and anode is also a part of stream flow control system. Usually we keep cathode outlet as 'open end' because most liquid water will be produced continually in cathode side during fuel cell operation, and it must be removed to prevent flooding problem. Exiting air is the most direct and efficient flow could carry out the liquid water. Also, air flow could remove the heat generated by fuel cell operation. In anode side, we use 'dead end' method to control the exiting flow because hydrogen is more valuable than air. Hydrogen flow is usually kept in anode until it is all consumed. But due to the back diffusion effect, a small part of liquid water produced in cathode will come to anode through membrane. So in order to purge the water out of anode, a purge valve will be placed at anode outlet. It will be closed in most time to keep the hydrogen consumed and open in a certain frequency to purge liquid water.

1.3.2 WATER MANAGEMENT SUBSYSTEM

How to manage water inside PEM fuel cell has been the major challenge of maintaining the PEM fuel cell stability. Low membrane humidity could significantly increase its resistance and reduce the fuel cell output voltage; moreover, operate at dehydration condition could shorten the fuel cell lifetime. On the other hand, liquid water on the gas diffusion layer could reduce the reaction area, cause fuel cell output voltage drop, or large amount of liquid water may even jam the gas flow channel, cause 'dead'

cell. So manage the liquid water, or humidification control, is the critical problem has to be solved if people want a more stable and long life fuel cell system.

1.3.3 THERMAL MANAGEMENT SUBSYSTEM

PEM fuel cell operation has to be operating in a certain temperature range in order to achieve high performance. Although the operating temperature of PEM fuel cell is the lowest among these major fuel cells and be able to achieve 'fast start up', it still needs to be heated up to a temperature which is higher than ambient temperature to stabilize the PEM fuel cell stack performance. On the other hand, PEM fuel cell is not a 100% efficient electricity power source. Most of the wasted energy (almost 50%) turns into heat during the fuel cell operation. If the heat produced by fuel cell operation cannot be removed, the fuel cell stack temperature will keep increasing. When the temperature is higher than PEM fuel cell operation temperature, the fuel cell performance is going to be decreased and fuel cell stack may be damaged by high temperature. Thus, a pre-heat system and cooling system are needed for thermal management subsystem to maintain the PEM fuel cell operating temperature.

1.4 PEM FUEL CELL-BATTERY POWER SYSTEM

A PEM fuel cell operates in low temperature condition is suitable for portable power application. However, PEM fuel cell has some problems working independently as power system. Rapid voltage drop and slow response to load demand are the major critical issues, because most electronic devices require stabilized power and fast transient response. Thus, energy storage devices like fast charge and discharge battery and power

regulation devices like DC/DC converters are needed to work with PEM fuel cell together to form a power system in order to provide regulated, fast-responded power to variable load.

1.4.1 POWER MANAGEMENT SUBSYSTEM

Power management system, as the major control system in PEM fuel cell-battery power system, directly controls the fuel cell stack sub-system, battery charging sub-system and power distribution control sub-system. How to design the power management system is one of the critical issues in optimizing the power system performance, efficiency and components life time.

1.5 LITERATURE REVIEW

1.5.1 PEM FUEL CELL SYSTEM MODELING AND CONTROL

For best understanding of the PEM fuel cell operation, PEM fuel cell modeling is needed to address PEM fuel cell system numerically. Basic concept of fuel cell and general mathematical model was introduced in books [1, 2, 3]. Up to now, many improved PEM fuel cell mathematical models have been published [4-12]. Most of these literatures are intended for PEM fuel cell steady-state simulation or sizing PEM fuel cell parameters. Due to the complexity and heavy calculative load of these models, they are not suitable for control design pursers. In order to control a PEM fuel cell system to operate at an optimal condition and to keep the fuel cell system high performance, a simplified, control-oriented model is needed for control design. Pukrushpan and Peng first developed a dynamic model which is suitable for the control study of fuel cell

systems in [13]. They did great job in simplifying the existing models, make it simple enough to address major PEM fuel cell transient and behavior, and in the same time greatly reduced the complexity and computational load. Their model ensured that control work on PEM fuel cell can be rapidly developed. Later, several improved control-oriented models were published [14, 15, 16]. They use the same principle to derive PEM fuel cell model and contribute either temperature effect model or humidifier model into control-oriented PEM fuel cell model.

After the control-oriented PEM fuel cell model was matured and widely implemented, control design on PEM fuel cell system is straight forward. All the known control methods can be applied on PEM fuel cell applications Lots of publicans has been released [13, 15, 17, 18] with different control strategy (linear, non-linear, fuzzy-logic, etc), or for different control purpose in fuel cell operation(flow control, humidity control, pressure control, etc).

1.5.2 PEM FUEL CELL-BATTERY POWER SYSTEM

As the major application of PEM fuel cell stack, PEM fuel cell- battery power system is wildy used in automotive or stationary application. PEM fuel cell-battery power system is discussed in many papers [19-29], including system design, modeling and power management system. But when they model the PEM fuel cell stack, they usually neglect the fuel cell thermal dynamic and use a PEM fuel cell equivalent circuit to represent PEM fuel cell model. This could reduce the complexity of the model but the thermal dynamic of fuel cell is the key part for PEM fuel cell performance. Neglecting

the thermal dynamic behaviour of fuel cell could lose a lot of model accuracy. PEM fuel cell–battery power systems in these literatures may have different topologies, but their power management strategies all have the similar philosophy, which is balancing the power distribution between fuel cell and battery to satisfy the load demand.

1.6 MOTIVATION

From the literature review of PEM fuel cell-battery power system we find out that control-oriented PEM fuel cell modeling is a matured technique, the existing model in [13] is good enough to address the known phenomenon in PEM fuel cell stack. But in their study, they only made assumption the humidity and temperature is perfectly controlled but they did not implement these two controllers. So in this study, we will design a humidification controller and a temperature controller for the PEM fuel cell system.

Also, the PEM fuel cell-battery power system model in previous literatures usually only has the PEM fuel cell electric model. To increase the accuracy of the system model, we are going to use a full set of PEM fuel cell stack model, and integrate with system auxiliaries models, to build a more accurate PEM fuel cell-battery power system model, which can be used as a platform for system control design.

Moreover, to our knowledge, the controllers designed before are either using lots of assumptions or based on a large amount of sensors to achieve data acquisition. That is because when they doing research, cost is not the major problem. They can build very nice experiment test bench with very expensive environment conditioner and sensors, and

then, the numerical results can be validated. This somehow deviate the goal of building an affordable alternative energy source. And their controller may not be working at a nature environment. Based on this concern, we are going to redesign all system controllers on purposes of control the fuel cell operation in natural ambient environment. Thus, a cost-efficient, practical (not test bench), portable PEM fuel cell-battery power system with embedded control system is needed for both numerical results validation and demonstration.

1.7 OBJECTIVE

- i. Based on the motivations above, the objectives of this study are listed below.
- ii. Introduce a set of PEM fuel cell-battery power system models for control design.
- iii. Develop a set of system controller to address all control issues in PEM fuel cell-battery power system, including fuel cell stack flow controller, humidification controller, thermal management controller and system power management system.
- iv. Develop an advanced power management system which has the function of extending the components lifetime and overload protection.
- v. Develop a real PEM fuel cell-battery power system with embedded controller.

1.8 THESIS OVERVIEW

PEM fuel cell-battery system fundamentals, literature review and motivation are explained in Chapter 1.

In Chapter 2, a control-oriented PEM fuel cell stack model based on [12, 13] is explained, and model simulation is presented. In Chapter 3, PEM fuel cell-battery power system auxiliaries models including battery model, DC-DC converter model and air blower are introduced.

In Chapter 4, system control algorithms including PEM fuel cell stack stream flow control, temperature control, water management system and PEM fuel cell-battery system power management system are designed. All numerical simulation results are shown in Chapter 4.

The design and building a portable PEM fuel cell-battery power system with embedded control system is introduced in Chapter 5. The portable PEM fuel cell-battery power system performance will be showed.

Chapter 6 will summarize and conclude this study; some suggestions and future work will be presented.

2. PEM FUEL CELL STACK MODEL

Many PEM fuel cell stack models were proposed before. These researchers did great contribution to PEM fuel cell modeling. Up to now, the best control-oriented PEM fuel cell stack model is done by Pukrushpan and Peng. They developed a simplified dynamic model which is suitable for fuel cell control study in [12]. In the paper temperature of fuel cell stack is assumed to be constant. This assumption greatly reduced the order of PEM fuel cell stack model, reduced the simulation time and complexity. On the other hand, the temperature of fuel cell stack can be controlled by a separate thermal management system. So this assumption is reasonable.

The PEM fuel cell stack model introduced in this study will be mainly based on their model.

A PEM fuel cell stack model consists two parts: PEM fuel cell thermal dynamic and electrochemical reaction.

2.1 PEM FUEL CELL FLOW DYNAMICS

In PEM fuel cell operation, thermal dynamic model is the major factor which dominates the fuel cell performance and stability.

In this model, mass conservation law is used here to address the mass flow rate of oxygen, nitrogen, and vapor in the cathode, and hydrogen, vapor in the anode [12].

2.1.1 MASS FLOW GOVERNING EQUATIONS

Mass conservation law is used here to derive the mass flow rate of oxygen, nitrogen, and vapor in the cathode, and hydrogen, vapor in the anode. [12].

In the cathode side, we have

$$\frac{dm_{O_2,ca}}{dt} = \dot{m}_{O_2,ca,in} - \dot{m}_{O_2,ca,out} - \dot{m}_{O_2,reacted} \quad (2.1)$$

$$\frac{dm_{N_2,ca}}{dt} = \dot{m}_{N_2,ca,in} - \dot{m}_{N_2,ca,out} \quad (2.2)$$

$$\frac{dm_{v,ca}}{dt} = \dot{m}_{v,ca,in} - \dot{m}_{v,ca,out} + \dot{m}_{v,ca,gen} + \dot{m}_{v,memberane} \quad (2.3)$$

In the anode side

$$\frac{dm_{H_2,an}}{dt} = \dot{m}_{H_2,an,in} - \dot{m}_{H_2,an,out} - \dot{m}_{H_2,reacted} \quad (2.4)$$

$$\frac{dm_{v,an}}{dt} = \dot{m}_{v,an,in} - \dot{m}_{v,an,out} + \dot{m}_{v,memberane} \quad (2.5)$$

We use electrochemical principle to calculate the rates of oxygen consumption $\dot{m}_{O_2,reacted}$, water production $\dot{m}_{v,ca,gen}$, and the hydrogen consumption rate $\dot{m}_{H_2,reacted}$ from the stack current, I_{st} .

$$\dot{m}_{O_2,reacted} = M_{O_2} \times \frac{ni_{st}}{4F} \quad (2.6)$$

$$\dot{m}_{v,ca,gen} = M_v \times \frac{ni_{st}}{2F} \quad (2.7)$$

$$\dot{m}_{H_2,reacted} = M_{H_2} \times \frac{ni_{st}}{2F} \quad (2.8)$$

where n is the number of cells in the stack and F is the Faraday number = 96485 C/mol.

2.1.2 STACK PRESSURE CHANGE

In this model we assume all gases flow the ideal gas law, temperature inside cathode and anode are equal to stack temperature [12]. Then we can calculate the partial pressure of oxygen, p_{O_2} , nitrogen, p_{N_2} , cathode vapor, $p_{v,ca}$, hydrogen, p_{H_2} , anode vapor, $p_{v,an}$, and relative humidity(ϕ), using ideal gas law based on masses of oxygen, m_{O_2} , nitrogen, m_{N_2} , cathode vapor, $m_{v,ca}$, hydrogen, m_{H_2} , anode vapor, $m_{v,an}$, and the stack temperature, T_{fc} .

In cathode, we have

Oxygen Partial Pressure:

$$p_{O_2,ca} = \frac{m_{O_2,ca} R_{O_2} T_{st}}{V_{ca}} \quad (2.9)$$

Nitrogen Partial Pressure:

$$p_{N_2,ca} = \frac{m_{N_2,ca} R_{N_2} T_{st}}{V_{ca}} \quad (2.10)$$

Vapor Partial Pressure

$$p_{v,ca} = \frac{m_{v,ca} R_v T_{st}}{V_{ca}} \quad (2.11)$$

Partial pressure of dry air in cathode:

$$p_{a,ca} = p_{O_2,ca} + p_{N_2,ca} \quad (2.12)$$

Total cathode pressure:

$$p_{ca} = p_{a,ca} + p_{v,ca} \quad (2.13)$$

In anode side, we have

Hydrogen Partial Pressure:

$$p_{H_2,an} = \frac{m_{H_2,an} R_{H_2} T_{st}}{V_{an}} \quad (2.14)$$

Vapor Partial Pressure

$$p_{v,an} = \frac{m_{v,an} R_v T_{st}}{V_{an}} \quad (2.15)$$

Total anode pressure:

$$p_{an} = p_{H_2,an} + p_{v,an} \quad (2.16)$$

2.1.3 RELATIVE HUMIDITY INSIDE STACK

Relative Humidity in cathode:

$$\phi_{ca} = \frac{p_{v,ca}}{p_{sat}(T_{st})} \quad (2.17)$$

Relative Humidity in anode:

$$\phi_{an} = \frac{p_{v,an}}{p_{sat}(T_{st})} \quad (2.18)$$

where p_{sat} is vapor saturation pressure, varying with temperature. In this model, T_{st} is a constant value, so vapor saturation pressure is also a constant.

2.1.4 WATER TRANSFER ACROSS MEMBRANE

The water transfer across membrane behavior is due to two major phenomena: the electro-osmotic drag from anode to cathode and back-diffusion from cathode to anode. Here we assume the water concentration, C_v , is changing linearly. We can use the following equation to capture this phenomenon

$$\dot{m}_{v,membrane} = M_v A_{fc} n \left(n_d \frac{i}{F} - D_\omega \frac{(c_{v,ca} - c_{v,an})}{t_m} \right) \quad (2.19)$$

where t_m (cm) is the thickness of the membrane. n_d is the electro-osmotic coefficient. D_ω is the diffusion coefficient, which varies with water content in the membrane, M_v is the vapor molar mass, A_{fc} (cm²) is the fuel cell active area, and n is the number of fuel cells in the stack [17].

The membrane water content λ_i is calculated by

$$\lambda_i = \begin{cases} 0.043 + 17.81a_i - 39.85a_i^2 + 36.0a_i^3 & (0 < a_i \leq 1) \\ 14 + 1.4(a_i - 1) & (1 < a_i \leq 3) \end{cases} \quad (2.20)$$

where a_i is the water activity, which can be calculated by

$$a_i = \frac{a_{an} + a_{ca}}{2} \quad (2.21)$$

The electro-osmotic and diffusion coefficients are calculated from

$$n_d = 0.0029\lambda_m^2 + 0.05\lambda_m - 3.4 \times 10^{-19} \quad (2.22)$$

And

$$D_\omega = D_\lambda \exp\left(2416 \left(\frac{1}{303} - \frac{1}{T_{fc}}\right)\right) \quad (2.23)$$

where

$$D_\lambda = \begin{cases} 10^{-6} & (\lambda_m < 2) \\ 10^{-6}(1 + 2(\lambda_m - 2)) & (2 \leq \lambda_m \leq 3) \\ 10^{-6}(3 - 1.67(\lambda_m - 3)) & (3 < \lambda_m \leq 4.5) \\ 1.25 \times 10^{-6} & (4.5 \leq \lambda_m) \end{cases} \quad (2.24)$$

T_{fc} is the temperature of the fuel cell.

2.2 ELECTROCHEMICAL MODEL

Electrochemical model is mainly used to address the electric property of the PEM fuel cell stack.

Fuel cell voltage model will be formed simply by subtracting three major over potentials from the open circuit voltage

$$V_{\text{cell}} = E_0 - V_{\text{act}} - V_{\text{ohm}} - V_{\text{conc}} \quad (2.25)$$

where E_0 is cell open circuit voltage, also been called thermodynamic potential, can be calculated by

$$E_0 = 1.229 - 0.85 \times 10^{-3}(T_{\text{fc}} - 298.15) + 4.3085 \times 10^{-5}T_{\text{fc}} \left[\ln(p_{\text{H}_2}) + \frac{1}{2} \ln(p_{\text{O}_2}) \right] \quad (2.26)$$

Activation over potential is caused by slow charge transfer reaction at the surface of the electrodes. Some of the electrode potential is used to drive the electron transfer to match the current demand and thus the potential at the fuel cell terminal is reduced.

Activation over potential V_{act} can be determined by

$$V_{\text{act}} = a \ln\left(\frac{i}{i_0}\right) \quad (2.27)$$

where i is current density. a and the exchange current density, i_0 , are all constants, which could be determined empirically.

Ohmic over potential occurs due to resistance to the flow of ions in the electrolyte, resistance to the flow of electrons through the electrodes and the contact resistance at the cell terminals. The ohmic over potential V_{ohm} can be determined by

$$V_{ohm} = iR_{ohm} = i \frac{t_m}{\sigma_m} \quad (2.28)$$

where R_{ohm} is the internal electrical resistance. t_m is the thickness of the membrane. The membrane conductivity, σ_m , can be calculated by membrane water content, λ_m , and fuel cell temperature T_{fc} .

The value of membrane water content λ_m varies between 0 and 14, which is respectively equivalent to the relative humidity from 0% to 100%.

$$\sigma_m = (b_{11}\lambda_m - b_{12}) \exp\left(b_2 \left(\frac{1}{303} - \frac{1}{T_{fc}}\right)\right) \quad (2.29)$$

where constants b_{11} , b_{12} and b_2 are usually determined empirically [12].

The concentration over potential occurs due to a decrease in the concentration of the reactants at the electrode-electrolyte interface. A steady supply of the reactants is required at the electrode-electrolyte interface to maintain the flow of electric current. Due to diffusion or convection problems in the electrolyte, the concentration of the reactants is not maintained at the initial level. This over potential v_{conc} can be calculated by

$$v_{conc} = i \left(C_2 \frac{i}{i_{max}}\right)^{c_3} \quad (2.30)$$

where c_2 , c_3 , and i_{\max} are constants that can be determined empirically. The i_{\max} is the limiting current.

Since individual cells are stacked up in series to form a stack, the stack voltage will be

$$V_{\text{st}} = n \times V_{\text{fc}} \quad (2.31)$$

where n is the number of cells.

2.3 AIR AND HYDROGEN SUPPLY MODEL

In this study, the air is assumed to be supplied to fuel cell stack cathode instantaneously by an electronic blower and the flow rate can be calculated as a function of required fuel cell current.

$$\dot{m}_{\text{ca,in}} = (1 + \omega_{\text{atm}})\dot{m}_{\text{dry air}} = (1 + \omega_{\text{atm}})\frac{1}{x_{\text{O}_2}}\lambda_{\text{O}_2}M_{\text{O}_2}\frac{nI_{\text{st}}}{4F} \quad (2.32)$$

where the λ_{O_2} is the oxygen excess ratio, ω_{atm} is the air humidity ratio.

The hydrogen is supplied from a hydrogen tank and controlled by a solenoid valve. The flow rate can also be calculated as a function of required fuel cell current

$$\dot{m}_{\text{an,in}} = \lambda_{\text{H}_2}M_{\text{H}_2}\frac{nI_{\text{st}}}{2F} \quad (2.33)$$

where the λ_{H_2} is the hydrogen excess ratio.

3. FUEL CELL-BATTERY POWER SYSTEM AUXILIARY MODEL

3.1 AIR BLOWER MODEL

The blower model introduced in this study is a general compressor/blow model from [2] to using pressure difference between blower inlet and outlet and blower efficiency to calculate power consumed by the blower.

The inlet and outlet temperatures and pressures are defined as T_1 , T_2 , p_1 and p_2 accordingly.

$$\frac{T_2}{T_1} = \left(\frac{p_2}{p_1}\right)^{\frac{\gamma-1}{\gamma}} \quad (3.1)$$

Where γ is the ratio of specific heat capacities of gas c_p/c_v , there are some assumptions to be used to simplify the calculation:

- i. The heat generated by mechanism is ignored.
- ii. The change of kinetic energy between inlet gas and outlet gas are negligible.
- iii. Gas specific heat at constant pressure c_p is considered constant during the compression process.

Under above assumptions, the enthalpy is the only state which is changed by the mechanical work, thus we have:

$$\dot{W} = c_p(T_2 - T_1)\dot{m}_{\text{gas}} \quad (3.2)$$

\dot{m}_{gas} is the mass rate of the compressed gas. In fact, above formula is the isentropic process, because in the real work the exit temperature will be higher than the isentropic temperature, so have the new temperature:

$$\dot{W}^* = c_p(T_2^* - T_1)\dot{m}_{\text{gas}} \quad (3.3)$$

Now, the \dot{W}^* and T_2^* are the real work of compression and real exit temperature, we can calculate the ratio between isentropic work and the real work is isentropic efficiency,

$$\eta_{\text{cp}} = \frac{\text{isentropic work}}{\text{real work}} = \frac{c_p(T_2 - T_1)\dot{m}_{\text{gas}}}{c_p(T_2^* - T_1)\dot{m}_{\text{gas}}} = \frac{T_2 - T_1}{T_2^* - T_1} \quad (3.4)$$

Combine (3.2) and (3.4), we have

$$\eta_{\text{cp}} = \frac{T_1}{T_2^* - T_1} \left[\left(\frac{p_2}{p_1} \right)^{\frac{\gamma-1}{\gamma}} - 1 \right] \quad (3.5)$$

And the temperature difference will be:

$$\Delta T = T_2^* - T_1 = \frac{T_1}{\eta_{\text{cp}}} \left[\left(\frac{p_2}{p_1} \right)^{\frac{\gamma-1}{\gamma}} - 1 \right] \quad (3.6)$$

Combine 3.2 and 3.6 we have

$$\text{Power} = \dot{W}^* = c_p \frac{T_1}{\eta_{\text{cp}}} \left[\left(\frac{p_2}{p_1} \right)^{\frac{\gamma-1}{\gamma}} - 1 \right] \dot{m}_{\text{gas}} \quad (3.7)$$

This calculated power is the mechanical power needed to raise the gas pressure. To calculate the electric power consumed by blower, we have to consider the efficiency between the driving motor and the turbine. In this study, the efficiency is set up to be 85% according to the AMETEK 3.0 BLDC 12VDC Low-Voltage Blower data sheet.

3.2 DC/DC CONVERTER MODEL

DC/DC converters are used to regulate the fuel cell output power by converting the rapid changing fuel cell output voltage to a stabilized level to meet the requirement of electronics. In this study, the selected fuel cell stack output voltage is less than 10 V. In order for us to use this power for a standard electronics, we choose to boost this voltage to 12 V, which is the nominal voltage for auto electronics and small portable electronic device. Thus, the 12 V boost DC/DC converter is chosen in this study. And its efficiency is assumed to be 85%.

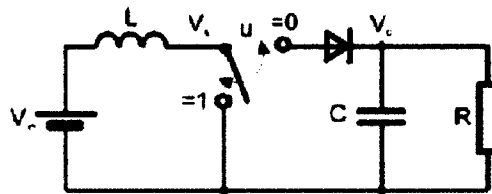


Figure 3. Boost DC/DC converter

Figure 3 shows the principle of a general switching boost DC/DC converter.

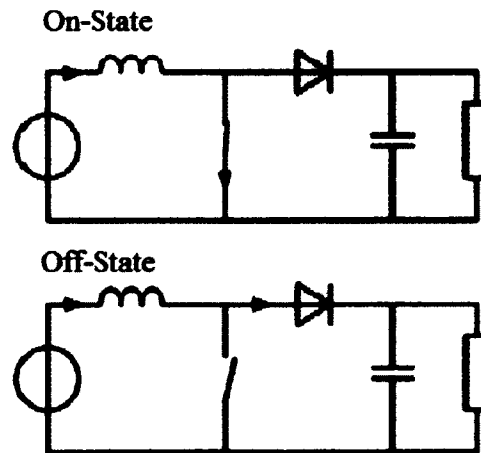


Figure 4. On-off state explained of boost DC/DC converter

The basic principle of a Boost converter consists of 2 distinct states (see Figure 4):

In the On-state, the switch (see Figure 4) is closed, resulting in an increase in the inductor current;

In the Off-state, the switch is open and the only path offered to inductor current is through the flyback diode, the capacitor C and the load R. That results in transferring the energy accumulated during the On-state into the capacitor.

Based on the basic principle of this DC/DC converter, a mathematical model can be derived as follow [19]

$$C \frac{dv_c}{dt} = (1 - u)i_L - \frac{v_o}{R} - i_o \quad (3.8)$$

$$L \frac{di_L}{dt} = v_o - (1 - u)v_o - R_L i_L \quad (3.9)$$

$$v_o = \frac{Rv_c}{R+R_c} + \frac{RR_c}{R+R_c} (i_L - i_o) \quad (3.10)$$

where the R_L is a body resistor of the inductor, R_c is an equivalent series resistor of the capacitor.

3.3 BATTERY MODEL

A generic battery model developed by Tremblay in [20] is a very simple battery model but can be used to capture the main behaviors of battery. Thus, the lithium-Ion battery model introduced in [20] is employed in this paper.

Discharge Model ($i_d > 0$)

$$f_1(Q_{\text{ext}}, i_d, i_{\text{batt}}) = E_0 - R \cdot \frac{Q}{Q - Q_{\text{ext}}} \cdot i_d - R \cdot \frac{Q}{Q - Q_{\text{ext}}} \cdot Q_{\text{ext}} + V_{\text{exp}} \cdot \exp(-Q_{\text{exp}} \cdot Q_{\text{ext}}) \quad (3.11)$$

Charge Model ($i_d < 0$)

$$f_2(Q_{\text{ext}}, i_d, i_{\text{batt}}) = E_0 - R \cdot \frac{Q}{Q_{\text{ext}} + 0.1 \cdot Q} \cdot i_d - R \cdot \frac{Q}{Q - Q_{\text{ext}}} \cdot Q_{\text{ext}} + V_{\text{exp}} \cdot \exp(-Q_{\text{exp}} \cdot Q_{\text{ext}}) \quad (3.12)$$

State of Charge (SOC)

$$\text{SOC} = 100 \left(1 - \frac{\int_0^t i_{\text{batt}} dt}{Q} \right) \quad (3.13)$$

where E_0 = Open circuit voltage (V)

R = Internal resistance (Ohms)

i_d = Low frequency current dynamics (A)

i_{batt} = Battery current (A)

Q_{ext} = Extracted capacity (Ah)

Q = Maximum battery capacity (Ah)

V_{exp} = Exponential voltage (V)

Q_{exp} = Exponential capacity (Ah)⁻¹

3.4 HUMIDIFIER MODEL

From the model predict results and some experiment study results, we know that since water is produced in PEM fuel cell cathode, the relative humidity in cathode side of the fuel cell stack always equal to 1. On the contrast, although water may come across membrane to anode side from cathode side duo to ‘back diffusion’ effect, when fuel cell operate at a high current density condition, the ‘electro-osmotic drag’ effect has much greater effect on water in anode and cause anode getting dryer and dryer. According to this phenomenon, a static model of the humidifier is placed between hydrogen control valve and fuel cell anode to humidify the supply hydrogen in order to humidify PEM fuel cell anode. Thus, a static humidifier model is needed to calculate the change in supply hydrogen humidity due to the additional injected water. The temperature of the flow is assumed to be constant as the ambient temperature. The water injected is assumed to be in the form of vapor, water two phase change is not considered here. We assume the flow goes into humidifier inlet has the same condition as at the hydrogen control valve. The pressure is the hydrogen tank outlet pressure, flow rate is the control valve outlet pressure, relative humidity is the same as the one from the hydrogen tank. Then, the thermodynamic properties can be calculate as :

vapor pressure is determined using Equation:

$$P_{v, \text{hum}} = \phi_{\text{hum}} P_{\text{sat}}(T_{\text{hum}}) \quad (3.14)$$

Since humid hydrogen is a mixture of hydrogen and vapor, hydrogen partial pressure is the difference between the total pressure and the vapor pressure

$$P_{\text{H}_2} = P_{\text{hum}} - P_{v, \text{hum}} \quad (3.15)$$

The humidity ratio can then be calculated from

$$\omega_{\text{hum}} = \frac{M_v P_{v,\text{hum}}}{M_{\text{H}_2} P_{\text{H}_2,\text{hum}}} \quad (3.16)$$

where M_{H_2} is the molar mass of hydrogen. The mass flow rate of hydrogen and vapor from the humidifier inlet is

$$\dot{m}_{\text{H}_2,\text{hum}} = \frac{1}{(1+\omega_{\text{hum}})} \dot{m}_{\text{hum}} \quad (3.17)$$

$$\dot{m}_{v,\text{hum}} = \dot{m}_{\text{hum}} - \dot{m}_{\text{H}_2,\text{hum}} \quad (3.18)$$

The mass flow rate of hydrogen remains the same for inlet and outlet of the hydrogen control valve. The vapor flow rate increases by the amount of water injected is

$$\dot{m}_{v,\text{hum}} = \dot{m}_{v,\text{hum}} + \dot{m}_{v,\text{inj}} \quad (3.19)$$

The vapor pressure change can be calculated by

$$P_{v,\text{hum}} = \omega_{\text{hum}} \frac{M_{\text{H}_2}}{M_v} P_{\text{H}_2,\text{hum}} = \frac{\dot{m}_{v,\text{hum}}}{\dot{m}_{\text{H}_2,\text{hum}}} \frac{M_{\text{H}_2}}{M_v} P_{\text{H}_2,\text{hum}} \quad (3.20)$$

The vapor pressure, $P_{v,\text{hum}}$, can then be used to determine the exit flow relative humidity

$$\phi_{\text{hum}} = \frac{P_{v,\text{hum}}}{P_{\text{sat}}(T_{\text{hum}})} = \frac{P_{v,\text{hum}}}{P_{\text{sat}}(T_{\text{hum}})} \quad (3.21)$$

Since the vapor pressure increases, the total pressure also increases. Thus

$$P_{\text{hum}} = P_{\text{H}_2,\text{hum}} + P_{v,\text{hum}} \quad (3.22)$$

The humidifier exit flow rate is governed by the mass continuity

$$\dot{m}_{\text{hum}} = \dot{m}_{\text{H}_2,\text{hum}} + \dot{m}_{\text{v},\text{hum}} = \dot{m}_{\text{H}_2,\text{in}} + \dot{m}_{\text{v},\text{hum}} + \dot{m}_{\text{v},\text{inj}} \quad (3.23)$$

4. PEM FUEL CELL-BATTERY POWER SYSTEM CONTROLS

The goal of design the PEM fuel cell-battery power system controller is to design a set of control algorithm can be applied on a low cost PEM fuel cell-battery power system; keep the system operation stable in a nature environment. The control system including PEM fuel cell stack flow control, thermal management, water management and system power management.

4.1 PEM FUEL CELL STACK FLOW CONTROL

4.1.1 AIR SUPPLY CONTROL

Previous studies have proposed all kinds of control strategy for PEM fuel cell air supply control. Most of their works are using different kinds of feedback control, which is taking system states by many sensors, design high robustness controller to tolerate system uncertainties. By doing this, the controller could theoretically perform very nice results, but it significantly increases the system cost and heave load calculation will not suitable for implemented into embedded controllers. On the other hand, by performing experiment we know the biggest challenge right now for causing PEM fuel cell unstable operation is liquid water problem, which is cannot be solved by model-base control along, because by far there is no non-CFD model can address the liquid water behavior in PEM fuel cell and CFD model cannot be used for control development. So according to our application, feed-forward control for air supply system is the best choose. The feed forward control in our application presents many advantages:

- i. It does not introduce instabilities.
- ii. It does not rely on measurements of the system's state, which in this particular

- case are much slower than the system's own dynamics;
- iii. It relies on a measurement of the system's only disturbance, I_{st} , which we can obtain inexpensively, with high precision and large bandwidth;
- iv. Reduce the computational load for embedded controller.

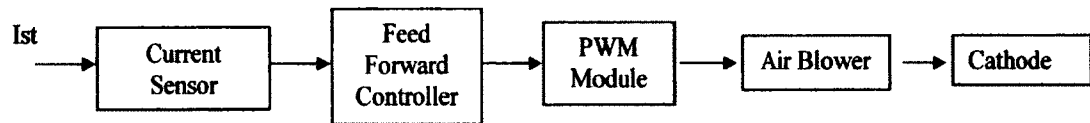


Figure 5. Feed forward control algorithm for PEM fuel cell air supply control

The feed forward control algorithm for air supply control is shown in Figure 5. The load required current can be measured by current sensor as a load following signal and convert into digital signal. The load following signal acts as the only input for feed forward controller. After calculation, the feed forward controller gives the PWM command through PWM module and directly controls the air blower speed so that the flow rate con cathode inlet can be controlled.

4.1.2 HYDROGEN FLOW CONTROL

Using the same principle as the air supply control, the hydrogen flow control can also be achieved by a simple feed forward controller. As shown in Figure 6

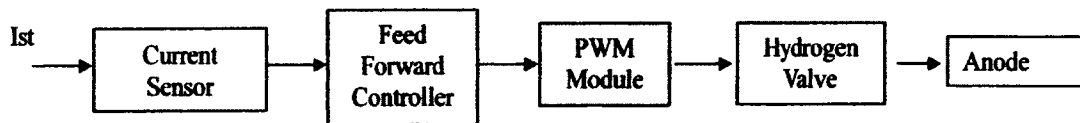


Figure 6. Feed forward control algorithm for PEM fuel cell hydrogen supply control

The feed forward coefficient can be calculated as a function of load following, I_{st}

$$\dot{m}_{an,in} = \lambda_{H_2} M_{H_2} \frac{nI_{st}}{2F} \quad (4.1)$$

where the λ_{H_2} is the hydrogen excess ratio.

By using feed forward controller for both cathode and anode flow control. We only need to use one sensor to complete both work.

4.1.3 SIMULATION OF PEM FUEL CELL STACK SYSTEM

After we applied the system input (air flow and hydrogen flow), we can see the simulation results of the PEM fuel cell stack system with integrated controller.

The parameters used in this simulation are based on a large PEM fuel cell stack, a 40kw fuel cell stack, so that we can see more clearly about the results.

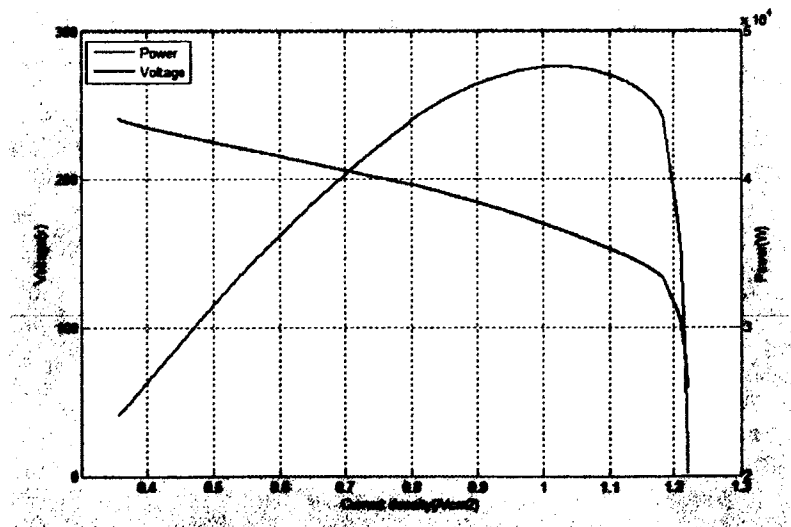


Figure 7. PEM fuel cell polarization characteristic

Figure 7 shows the PEM fuel cell polarization characteristic curve from simulation. This curve captures the real PEM fuel cell polarization behavior. The voltage curve decreases as the fuel cell current density goes high due to the three major voltage overpotential. The power curve is the product of fuel cell current and voltage. So it first increases as the current density increases, but when the current density reaches a point, it start to decrease because the output voltage decreases too much, and eventually goes to zero when the output voltage goes to zero.

A serial step input signal (shown in Figure 8) is employed here as the system input to test the fuel cell stack system model. With this input, we can investigate the fuel cell voltage response to current demand and the fuel cell transient.

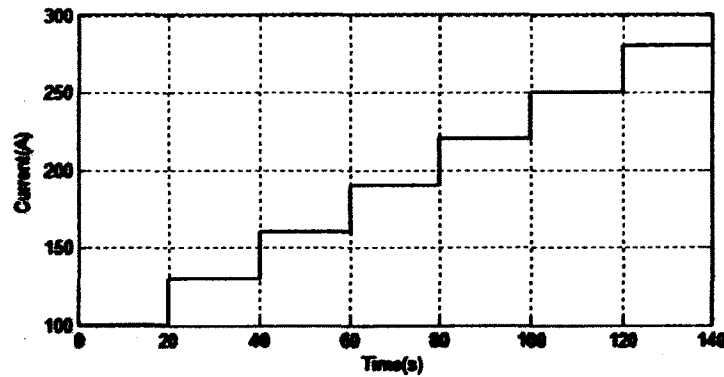


Figure 8. Serial step load input

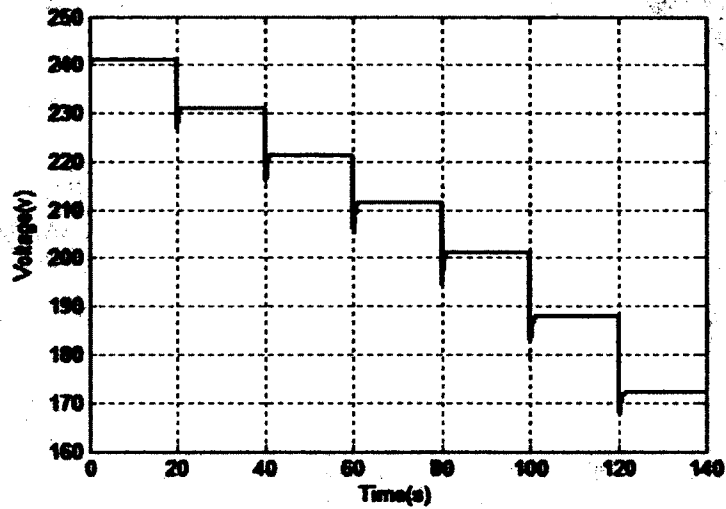


Figure 9. Voltage response to step input

The fuel cell output voltage response to the step input is shown in Figure 9. As the current input goes high, the output voltage decreases.

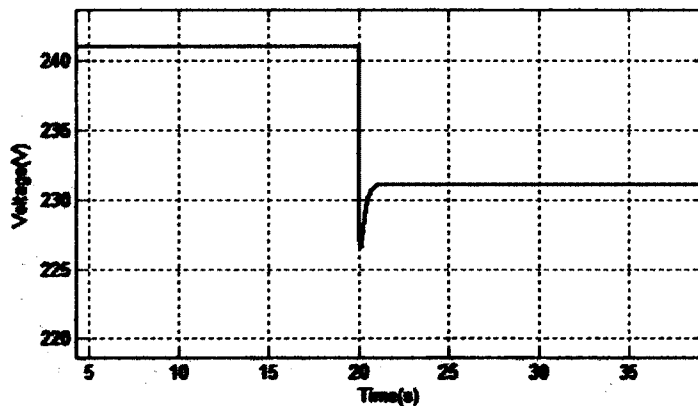


Figure 10. Output voltage transient when input current change from 100A to 130A

PEM fuel cell voltage transient response is shown in Figure 10. This Figure shows the fuel cell voltage response during the external load change. We can see from this Figure, when the input data change from 100A to 130A the voltage does not reduce to a

steady level. Instead, it drops to a lower point and recovers to a steady level after a period of time. This phenomenon is caused by the slow fuel cell transient response.

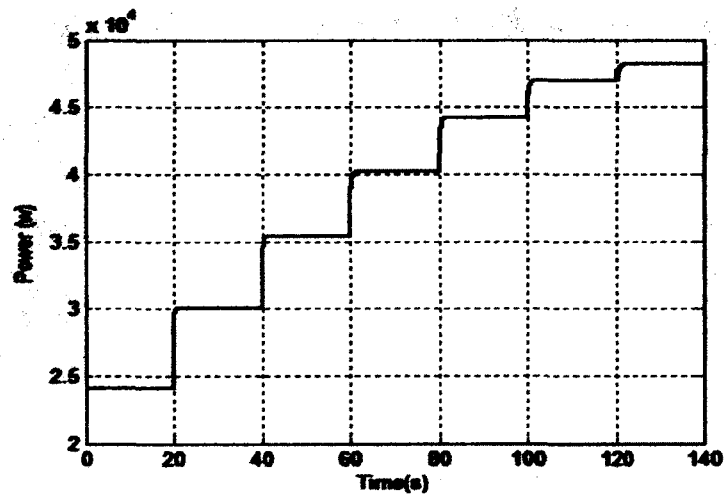


Figure 11. PEM fuel cell output power response

Figure 11 shows the fuel cell output power response due to the current step input. We can see that the power response is increasing but the interval tends to be smaller. That is because as the demanded current increase, the output voltage keeps going down. So since the power is the product of current and voltage, its increasing speed is decreasing.

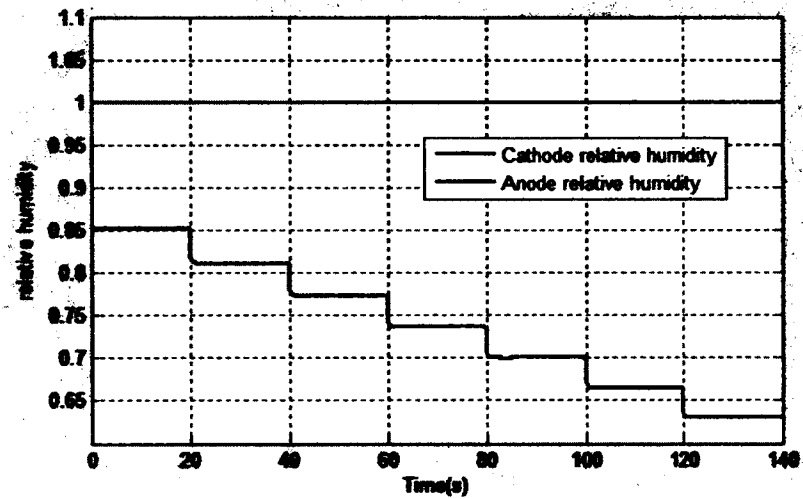


Figure 12. Relative humidity change due to step current input

Figure 12 shows the relative humidity change due to the step current input. Relative humidity is an important parameter which directly affects the fuel cell output voltage. We can see in fuel cell anode, the RH is getting lower as the current density goes high. This is because the electro-osmotic drag force is higher than the diffusion drag when the current density goes high. The water tends to go from anode to cathode. Also there is water produced during the fuel cell operation, so the RH in cathode is always equal to one. This curve can be used in humidification control of the fuel cell operation.

4.2 HUMIDIFICATION CONTROL

PEM fuel cell stack humidification control consists of two parts: liquid water control and humidifier control.

4.2.1 LIQUID WATER CONTROL

As mentioned in previous chapters, liquid water problem is the most crucial problem in keeping the PEM fuel cell operation from stable. Keeping a Little amount of liquid water on the membrane could maintain the membrane well humidified, than no extra humidifier is needed. But on the other hand, liquid water could easily jam the gas flow channel, cause dead cell, and reduce PEM fuel cell performance and life time. By far this is no general mathematical model could predict liquid water behaviour during PEM fuel cell stack operation.

Using model based control to deal with liquid water problem in PEM fuel cell is not a possible way due to the current technology. But using experimental-based study to find fuel cell stack input-output behaviour may be a solution to deal with liquid water. Jixin Chen has done an experimental study on a 10 cell PEM fuel cell stack in his master's thesis. From his results of output voltage response to a step input, we can see the output voltage has large vibration when input has already in constant value. By analysis this results, we eliminate all the possibilities, and we believe this vibration is caused by liquid water jammed channel.

This phenomenon gives us a possible solution for removing the liquid water from fuel cell stack. By keep doing experiment, we may find the pattern of the time of liquid water accumulation. If we can find that frequency, we can control the cathode blower to give a sudden pressure rise to push out the accumulated water. For the anode side, liquid water amount is not as much as cathode side; we may set up a constant purging time for the purge valve. It will do the work.

4.2.2 FEEDBACK CONTROLLER FOR HUMIDIFIER

According to Ohmic over-potential, the element could affect the membrane water content is activity a_{an} and a_{ca} . For water vapor case, the activity is equal to relative humidity inside cathode and anode. After simulation we can see the RH inside cathode is always equal to 1 because of water generation, so maintain the RH inside anode is the main issue for humidifier. Due to this conclusion, a feedback controller is designed to use the anode humidity as the feedback terms to calculate how much water should be injected to maintain itself well humidified (shown in Figure 13).

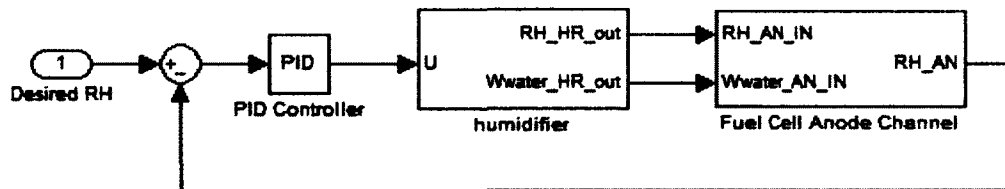


Figure 13. Humidification controller block diagram

4.2.3 SIMULATION RESULTS OF HUMIDIFIER CONTROL

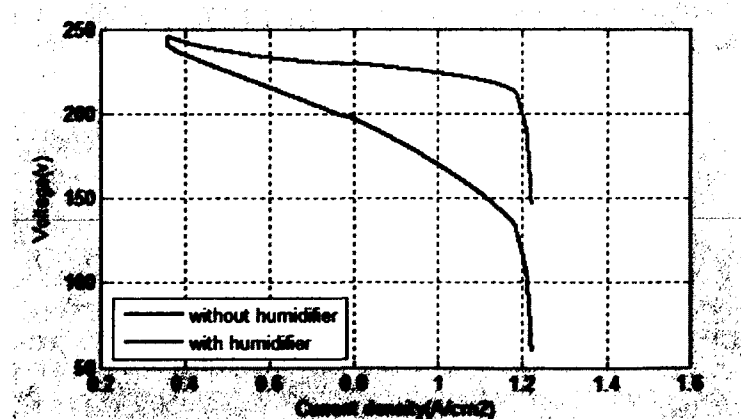


Figure 14. Polarization curve with and without humidifier control

In Figure 14 we can see the polarization characteristic with humidifier is much better than the condition without humidifier. The voltage output with humidifier per current density is higher than the output without humidifier

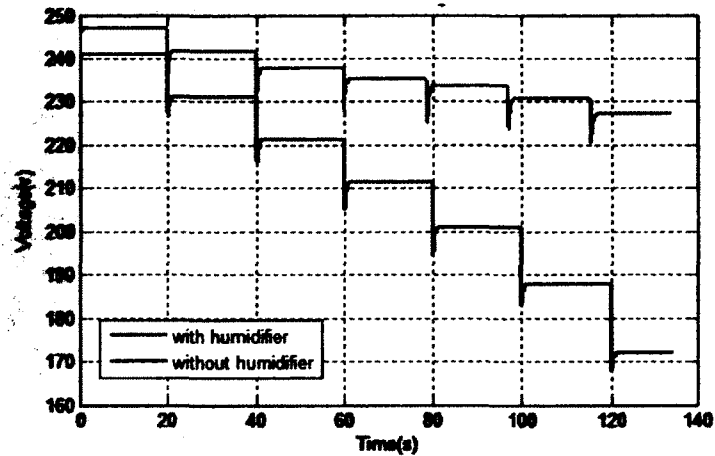


Figure 15. Output voltages with and without humidifier control

Figure 15 shows the fuel cell output voltage with and without humidifier. We can see the fuel cell output voltage with humidifier is higher than the one without humidifier control. This is because the Ohmic voltage loss tends to be higher when relative humidity inside the fuel cell stack is lower.

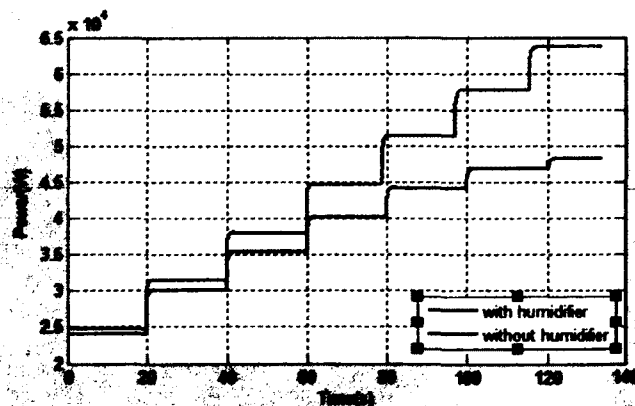


Figure 16. Output powers with and without humidifier control

The system output power with and without humidifier is shown in Figure 16. It basically follows the same behaviour as voltage.

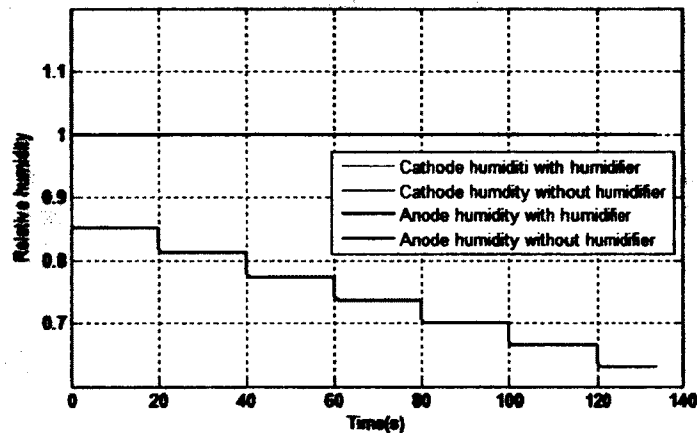


Figure 17. Relative humidity with and without humidifier control

The relative humidity inside fuel cell stack with and without humidifier is shown in Figure 17. We can see when the system running without humidifier, the cathode humidity is 1 because the water drag force and there is water generated in cathode. In the anode side, the water is dragged into the cathode side, so the relative humidity is keep going low as running. But when the humidifier is added, the relative humidity in both cathode and anode are equal to 1. This is because when the anode relative humidity goes low, the controller will control the humidifier to inject water into anode side.

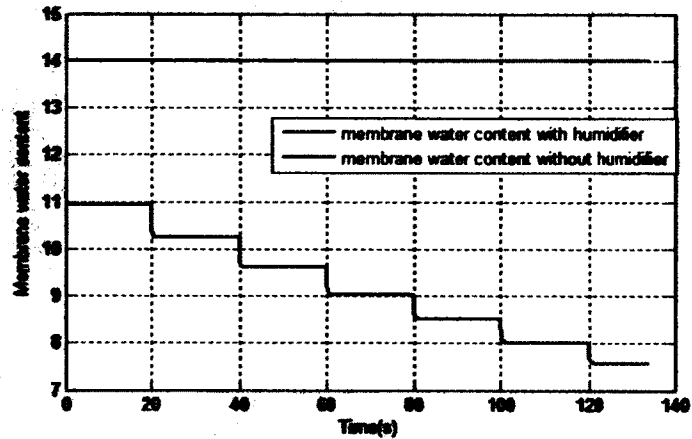


Figure 18. Membrane water content with and without humidifier control

As explained in equation 2.21-2.23, the relative humidity inside cathode and anode will be averaging to calculate the membrane water content, and the membrane water content is the actual factor that affects the fuel cell output voltage. As shown in Figure 18. The membrane water content with humidifier can always equal to 14, which means the membrane is 100% humidified. On the other hand, the membrane water content without humidifier keeps decreasing. This causes the big voltage drop during fuel cell operation.

4.3 PARAMETRIC STUDY OF PEM FUEL CELL STACK SYSTEM

Using the developed fuel cell stack model, we can conduct a parametric study on the fuel cell stack system.

In this set of simulation, we use a 100W PEM fuel cell stack with 10 cells and the cross section of 50cm².

A step current signal (shown in Figure 19) is used as system input in this section.

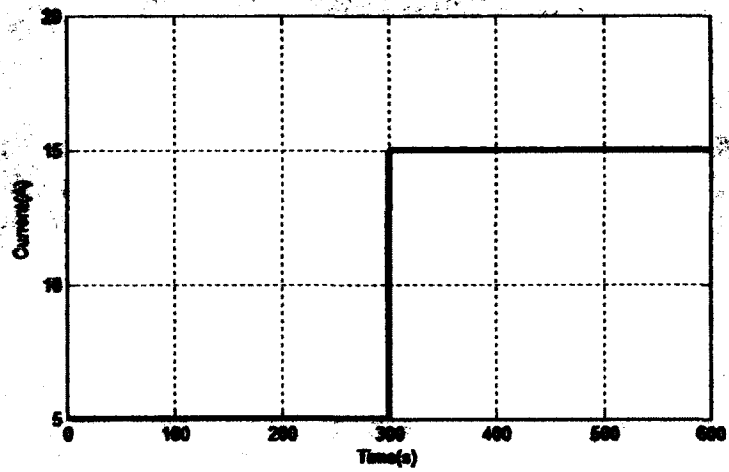


Figure 19. Step signal input for parametric study

4.3.1 TEMPERATURE EFFECT

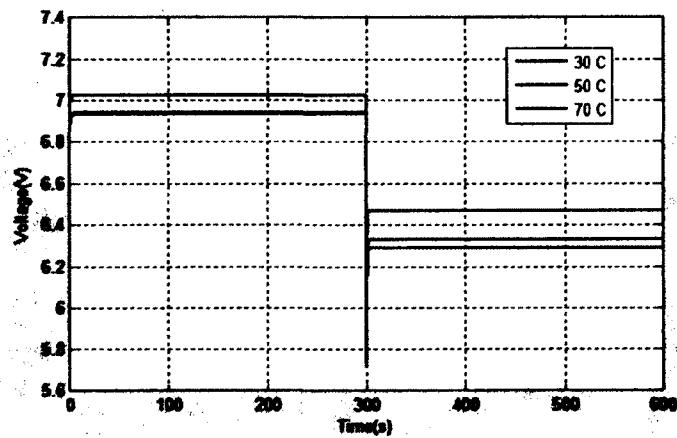


Figure 20. Fuel cell voltage response in different stack temperature

We can see from Figure 20 that the stack temperature has a proportion effect on fuel cell output voltage. As fuel cell stack operates under a high temperature has the higher output voltage than operates in the low temperature.

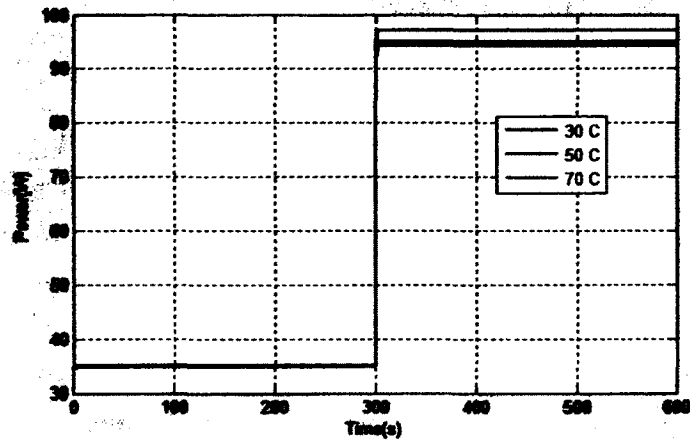


Figure 21. Fuel cell power response in different temperature

Since the fuel cell output voltage is higher in the high stack temperature condition, the fuel cell output power is higher in the high stack temperature condition than the low stack temperature (shown in Figure 21).

4.3.2 RELATIVE HUMIDITY EFFECT

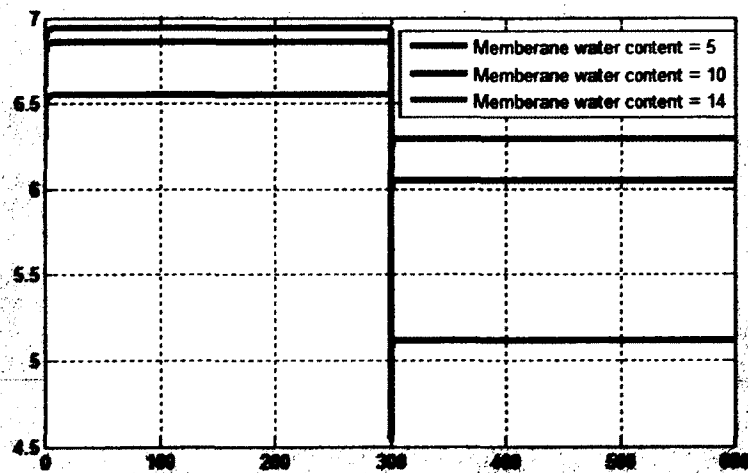


Figure 22. Fuel cell output voltage in different membrane water content

As explained in equation 2.21-2.23. The relative humidity in cathode and anode will be averaged to membrane water content, and this membrane water content is the factor that affects the fuel cell output voltage. So in this study we alternate the effect of relative humidity to membrane water content effect.

In Figure 22 the fuel cell output voltage is higher when the membrane water content equal to 14, which means the membrane is 100% humidified.

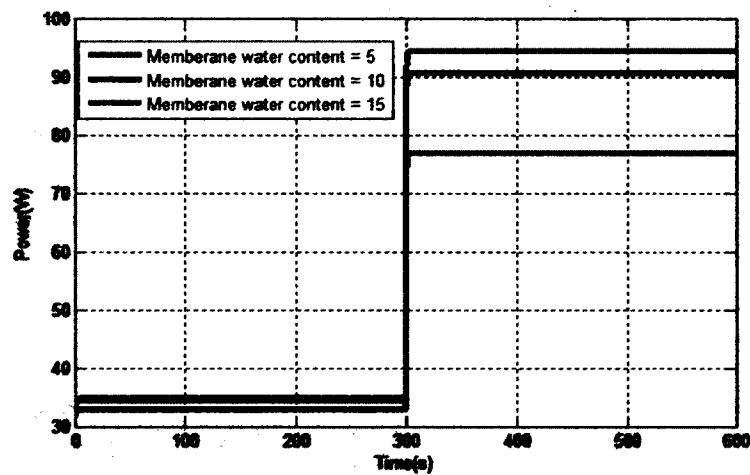


Figure 23. Fuel cell power response in different membrane water content

As the fuel cell output voltage is higher when the membrane water content is higher, the fuel cell output power is higher.

4.3.3 CATHODE INLET PRESSURE EFFECT

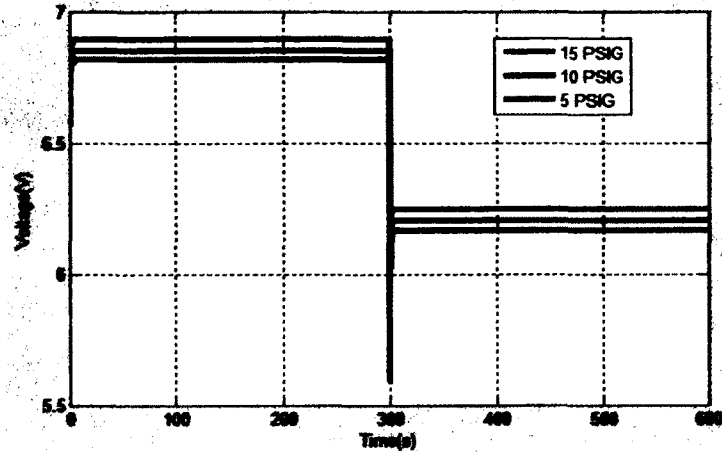


Figure 24. Fuel cell voltage response in different cathode inlet pressure

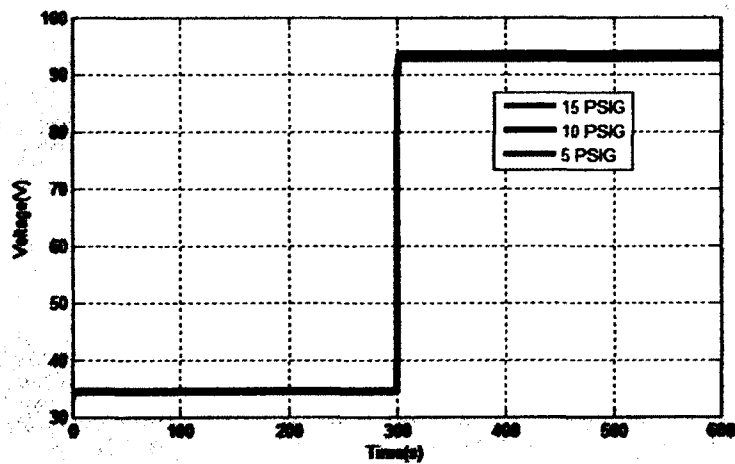


Figure 25. Fuel cell power response in different cathode inlet pressure

Cathode inlet pressure directly influences the oxygen partial pressure inside fuel cell stack cathode. It has proportional effects on fuel cell output voltage and power.

4.3.4 OXYGEN EXCESS RATIO EFFECT

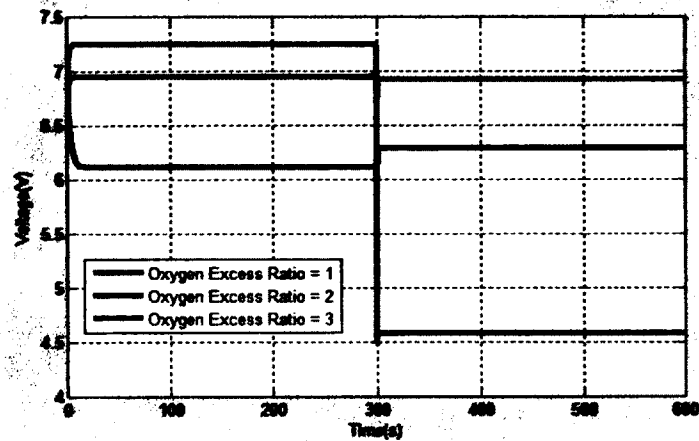


Figure 26. Fuel cell voltage response in different oxygen excess ratio

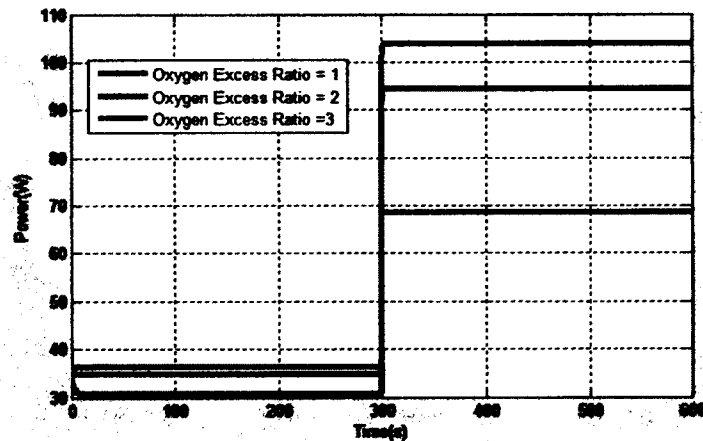


Figure 27. Fuel cell power response in different oxygen excess ratio

Oxygen excess ratio is the ratio between the supplied oxygen and reacted oxygen. The bigger oxygen excess ratio number means more oxygen is supplied into fuel cell cathode, this extra amount of oxygen can increase the oxygen partial pressure, thus increase the fuel cell output voltage and power (as shown in Figure 26-27).

4.4 POWER MANAGEMENT OF PEM FUEL CELL-BATTERY POWER SYSTEM

In this study, the power management algorithm is proposed based on the following rules:

When the load-required power is lower than the fuel cell-battery system rated power, which is 100 W in this study, the fuel cell will be employed to supply sufficient power to load. The battery will be only used to supply power to system auxiliaries. If the battery state of charge (SOC) is lower than its set lower bound, the fuel cell will start to charge the battery until the SOC reaches its set upper bound. During the charging time, system auxiliaries are powered directly by fuel cell.

When the load-required power is higher than the system rated power but lower than 150% of the system rated power, the battery will be controlled to supply power to the load simultaneously with fuel cell. The battery will not be charged no matter whether the SOC is lower than the set lower bound or not. System auxiliaries are powered by battery at all time.

When the load-required power is higher than 150% of the fuel cell-battery power system rated power. The system will automatically shutdown the connection to load to prevent damage to both load device and fuel cell-battery power system.

4.4.1 SIMULATION CONDITIONS

All the mathematical models introduced above have been implemented into the Simulink environment.

In order for us to capture the battery charging behavior in a short simulation time, a 12 V, 0.1 Ah lithium-ion battery is used here. According to the conclusion made by Kato in [20], the ideal SOC of lithium-ion battery should be kept around 60% to extend its life time. So in this study we choose the SOC upper bound to be 60%, the lower bound to be 58% and the initial SOC is 60%.

The auxiliary-consumed power is the sum of power consumed by blower, solenoid valves and microcontroller. The microcontroller consumed power is assumed to be 5 W as long as the operation continues.

4.4.2 RESULTS AND DISCUSSION

In this simulation, a series of step signals is used to represent the load-required power, which is the input of the system, is shown in Figure 28. This load-required power signal dry here captures all some major situation the system could encounter in the real application. At time 0 s, the load starts to require power from power system at 10 W. At 5 s, the required power increase to 60 W. At 10 s, the required power reaches the power system rated power 100 W. The first overload power, 140 W, starts at 15 s, but it is still within the system affordable power range, which is 150% rated power. At 20 s, the

required power becomes stable at rated power 100 W until 30 s. At 30 s, the second overload power 180 W comes, which exceeds the 150% of the system rated power limit.

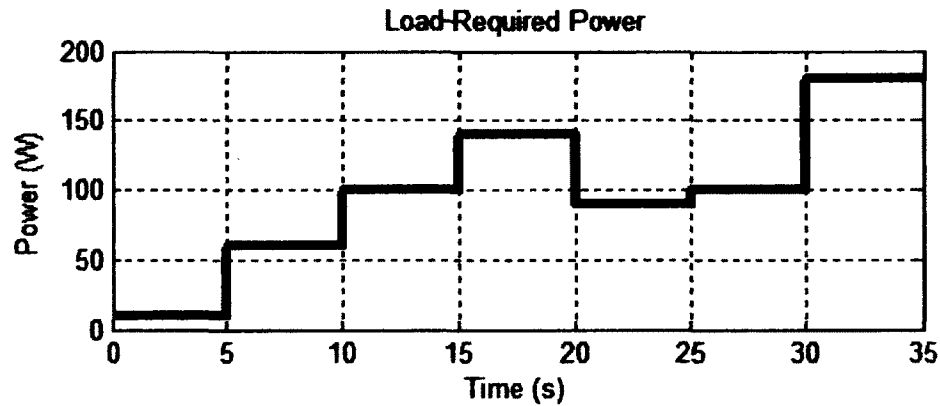


Figure 28. Load-Required Power

The simulation results are shown in Figure 29-36.

Figure 29 shows the fuel cell required current is calculated by the power management system and sent to fuel cell stack sub-system as an input. The fuel cell stack sub-system takes the required current as input and generated fuel cell voltage and power, shown in Figure 3. The fuel cell voltage will be regulated by DC/DC converter to a constant 12 V, and fuel cell produced power will be reduced by 15% due to the efficiency of DC/DC converter. The regulated DC power and voltage is shown in Figure 31. The battery power is shown in Figure 32. The positive power represents the battery is supplying power and the negative number means the battery is under charging process. According to the battery power situation, the SOC is shown in Figure 33. The system

auxiliaries consumed power along with time is shown in Figure 34. The system overall output power versus the load-required power is shown in Figure 35.

We can see from the results that in the first 5 seconds, the load-required power is only 10 W and only the fuel cell provides the power to the load. At 5 s, the load-required power increased to 60 W. The required fuel cell power increased, thus the battery power consumed by blower increased. At 5.2 s the battery SOC reached the lower bound 58% and the battery started to be charged. The fuel cell produced power increased in the same time in order to charge the battery and supply the auxiliaries. At 8 s, the battery SOC was charged to 60% so the fuel cell stop charging the battery and the battery started to supply the auxiliaries again. At 10 s, the load-required power increased to the system rated power 100 W. The fuel cell could still sufficiently supply the load-required power and charge the battery during this process. At 15 s, the load-required power

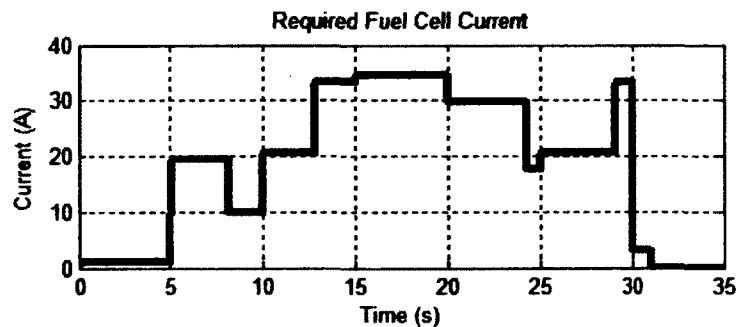


Figure 29. Required Fuel Cell Current

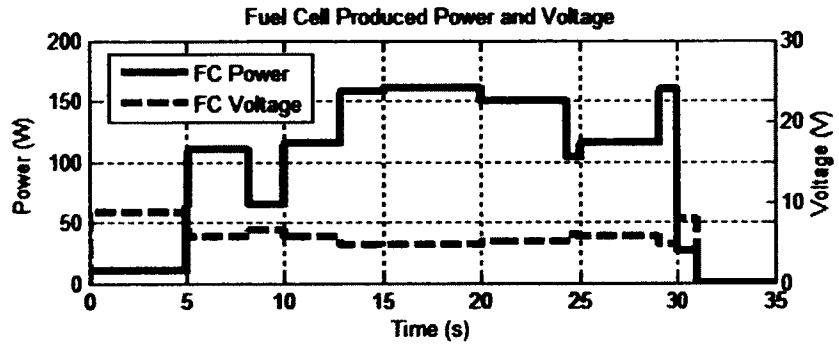


Figure 30. Fuel Cell Produced Power and Voltage

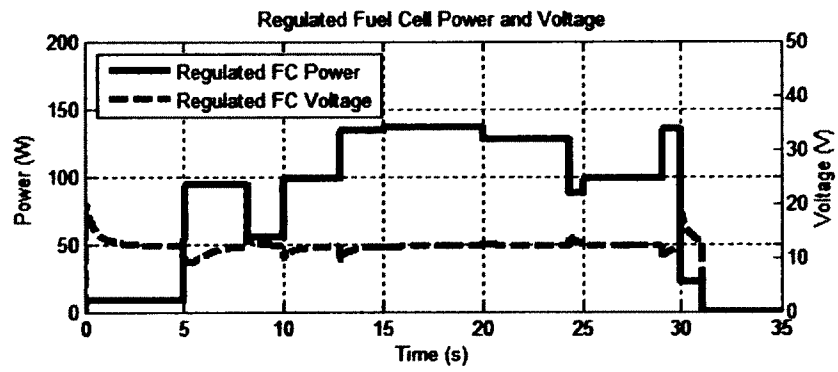


Figure 31. Regulated Fuel Cell Power and Voltage

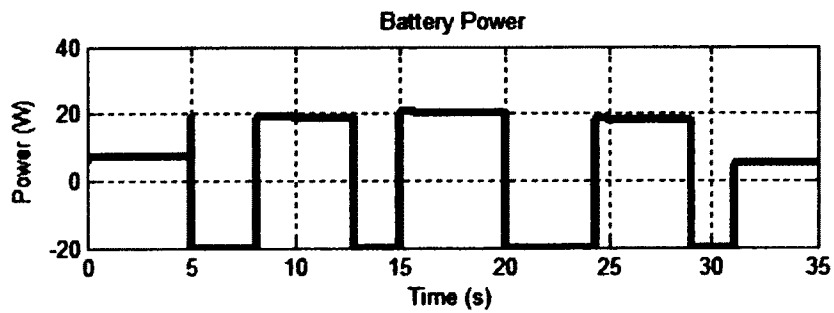


Figure 32. Battery Power

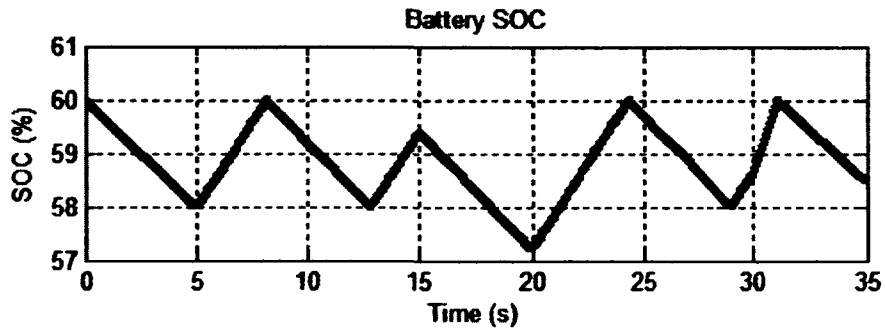


Figure 33. Battery SOC

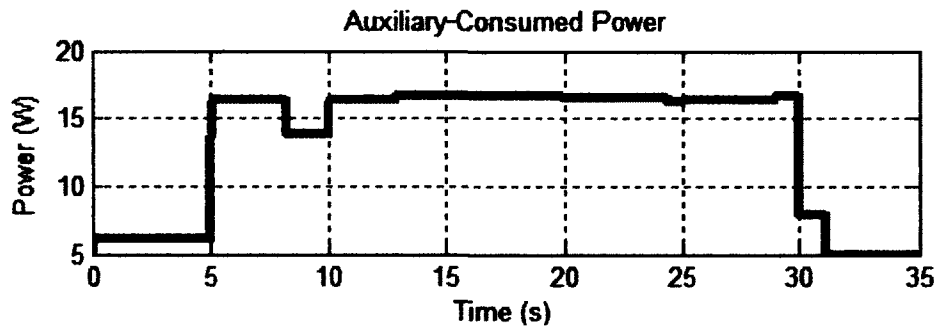


Figure 34. Auxiliary-Consumed Power

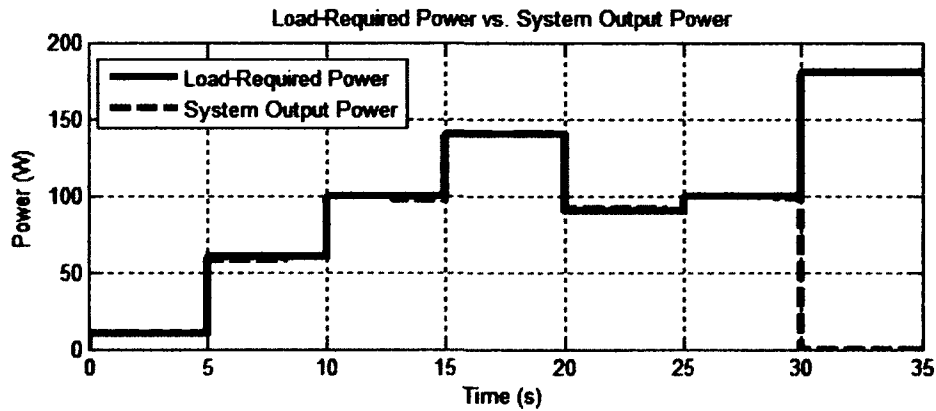


Figure 35. Load-Required Power vs. System Produced Power

increased to 140 W, which is 40% higher than the system rated power. During this situation, the fuel cell is not able to provide enough power for the load, so the power

management controls the battery to supply power to the load simultaneously with fuel cell. In 18 s even the SOC is lower than the lower bound 58%, the battery was still not charged because the power management considered supplying the load-required load as the priority. At 20 s, the load-required power reduced to 90 W, which is lower than the system rated power, the fuel cell starts to charge the battery because its power is sufficient at that moment. For the next 10 seconds the load-required power is kept with the system rated power so the system runs in a stable process. At 30 s, 180 W power is required by the load, which is more than 150% of the power system rated power. So in order to protect both the load device and the system, the overload emergency shutdown process is launched. The power system stopped providing power to the load. The fuel cell only provided power to battery if it is needed to be charged, and the only power-consuming device is the microcontroller.

5. PORTABLE PEM FUEL CELL-BATTERY SYSTEM WITH EMBEDDED CONTROL SYSTEM

5.1 SYSTEM EXPLAINED

A 100W portable PEM fuel cell-battery system is built in this study to validate the designed controller performance, and for investigate the PEM fuel cell performance.

A Portable PEM fuel cell-battery power system diagram is shown in Figure 36. In this system, a microcontroller is employed as the 'Brain' of this system. The microcontroller will take the demand current as an input, use power management algorithm to calculate the power distribution. PEM fuel cell stack will be controlled by blower and hydrogen control valve. Battery charge or discharge will be controlled by a switch. Temperature sensors is placed within this system and micro controller monitors the system temperature through these sensors and send control signal to a cooling fan to control the system temperature.

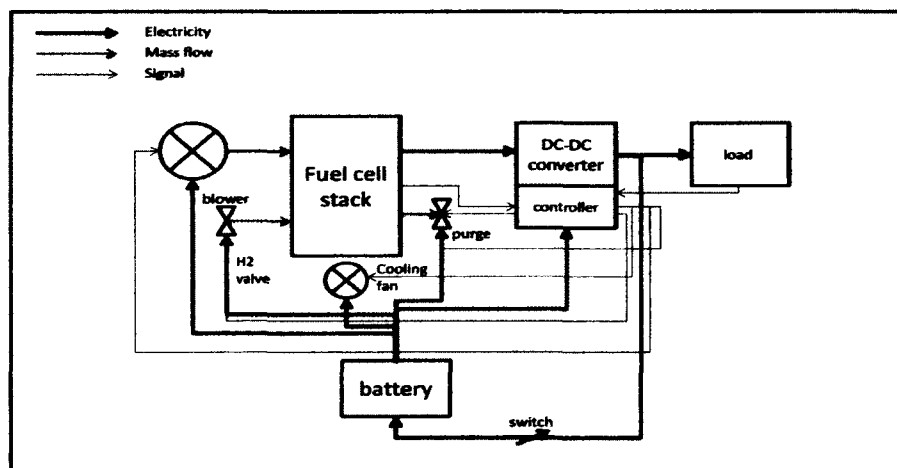


Figure 36. Portable PEM fuel cell-battery power system diagram

5.2 EXPERIMENTAL STUDY ON SIMULATION RESULTS VALIDATION AND PORTABLE PEM FUEL CELL-BATTERY SYSTEM PERFORMANCE

5.2.1 VALIDATION OF PEM FUEL CELL CONTROL SYSTEM SIMULATION

In this study, the 100W PEM fuel cell battery-power system with embedded control system is used to validate the simulation results. The fuel cell stack we used here is a 100W PEM fuel cell stack with 10 single cells and the cross section area of 50cm².

The simulation environment is set up as the experimental environment:

- i. Room Temperature
- ii. Initially well humidified stack by injecting liquid water
- iii. Same inlet initial pressure and ambient outlet pressure

The system input for simulation and experiment are shown in Figure 37 A step current signal is employed again in here. We choose low current density zone to test the fuel cell stack so we can get more accurate and clear results by minimize the uncertainties like fast temperature and relative humidity changing.



Figure 37. Step current input for simulation and experiment

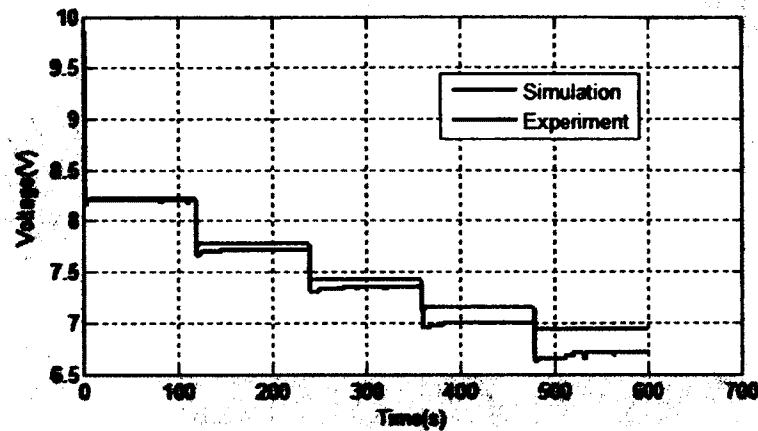


Figure 38. Voltage output for simulation and experiment

Figure 38 shows the voltage output of the system for simulation and experiment. We can see the simulation result follows the trend of the experiment result. They match each other in the first current 1A because in the initial state, all condition in simulation and experiment can be consider the same as we set up. As the demand current increase, the experiment result starts to go lower than the simulation result. The gap between the simulation results and the experiment result is increasing. This phenomenon is caused by two aspects: (1) as the experiment goes on, the relative humidity inside fuel cell stack is going lower and lower, thus the output voltage decreases more than the simulation results. The decreasing relative humidity also causes the fuel cell operation response time to go slower. (2) In the experiment, we use a 12VDC 2Amp blower as the air supply tool. The maximum output pressure of this blower is 0.5 PSI, which meets the minimum requirement for this fuel cell stack. But the fuel cell stack has a very thin, long channel, it causes very much pressure drop. So the actual cathode pressure is much lower than the blower output pressure. When the demand current is 1A, the flow rate input of the fuel cell stack is sufficient, but when the demand current goes up, the fuel cell will not have

enough oxygen as reactant. Thus the experiment output voltage decreases faster than the simulation results. This problem can be solved by changing a high pressure blower, but the bigger blower will consume more power than the current one. Since the blower power is provided by the fuel cell stack output power, it has a power limit of 100W, theoretically. Up to now, we cannot find a 12v blower which can provide up to 5PSIG pressure and consume less than 100W power.

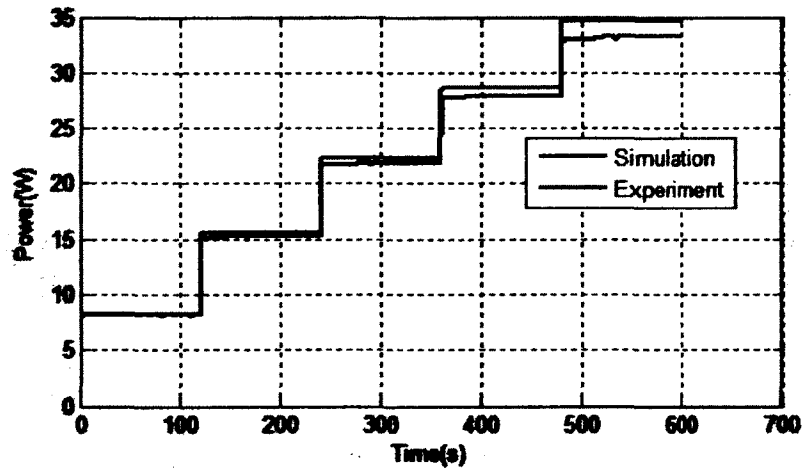


Figure 39. Power output for simulation and experiment

Figure 39 shows the power output for simulation and experiment. It follows the trend of the system voltage output. The increasing speed of experiment result is getting slower than the simulation results. It is also caused by air starvation and low relative humidity.

5.2.2 PORTABLE PEM FUEL CELL-BATTERY POWER SYSTEM PERFORMANCE

The purpose of building a 100W portable PEM fuel cell-battery power system is to use the PEM fuel cell stack as the main power source to provide continuous regulated DC power to electronics. So in the testing of power system, we are going to test the regulated DC power output from the PEM fuel cell-battery power system. The expected results should be a constant 12VDC output voltage which is not affected by the current demand like the fuel cell stack system did, so this result does not require a simulation results validation.

A step current signal (shown in Figure 40) is used in this experiment study as the system input.

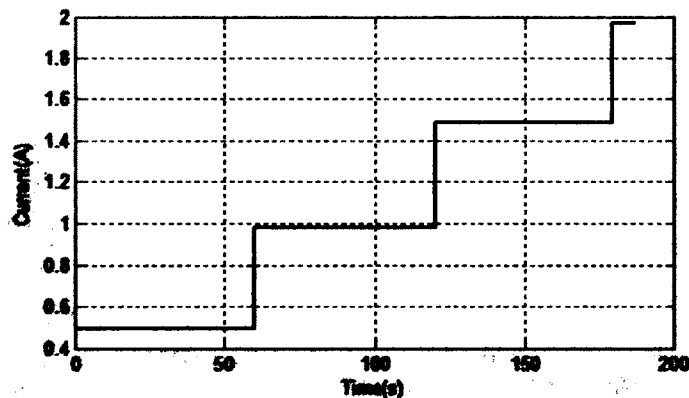


Figure 40. Step current demand input

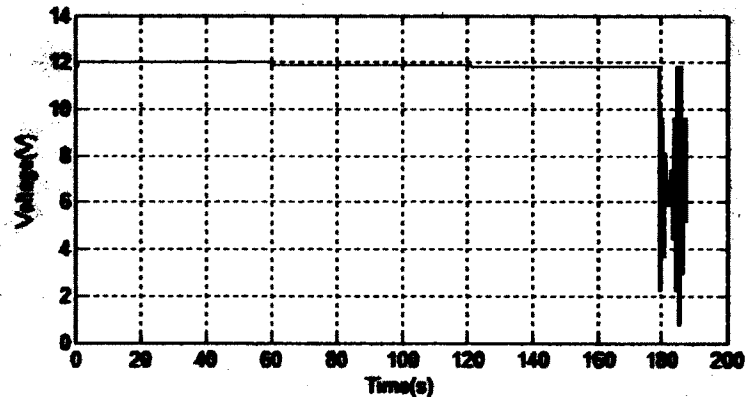


Figure 41. System voltage output

The Figure 41 shows the system voltage output of the power system. We can see for the first 180s the system output voltage is between 12V and 11.8V which is acceptable for most electronics. But start from 180s, the system output become unstable. This is caused by the property of the DC/DC converter. The DC/DC converter we used here accepts input voltage from 6-19VDC and the efficiency is around 80% when the input voltage is between 9V-15V. When the current demand at the DC/DC converter output is 2A, the actual current demand of the fuel cell stack is 5 A or even more because the fuel cell stack output voltage at this time is around 7V, the DC/DC converter efficiency goes to non-linear zone, which can be less than 30%. The more current demand on fuel cell stack, the lower the fuel cell stack voltage becomes. When the fuel cell stack output voltage is lower than 6V, the DC/DC converter stops running. As far as we know, not commercial DC/DC converter could accept input voltage lower than 6V because physically converter that lower voltage to a high voltage will cause huge power loss during the process. So the solution is either build a DC/DC converter or use a fuel cell stack which can provide higher output voltage.

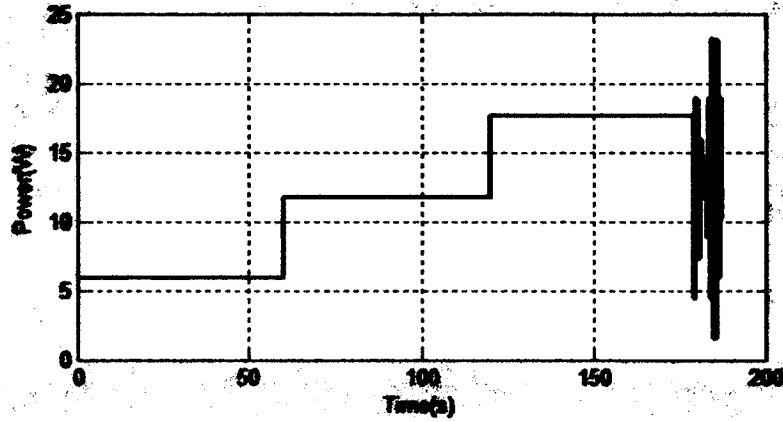


Figure 42. System power output

Figure 42 shows the fuel cell-battery power system output power. We can see due to the limitation of low voltage output of fuel cell stack, the system output cannot be higher than 18W. But as a demonstration project, this results shows the system can provide a continuous 12VDC power to electronics as a power source.

6. CONCLUSIONS AND RECOMMENDATIONS

6.1 CONCLUSIONS

In this study, a general methodology of modeling, control and building a proton exchange membrane fuel cell-battery power system is developed. A set of PEM fuel cell-battery power system model is introduced. This model can be used to address the transient of the PEM fuel cell-battery power system as well as to be used as a platform for system controller development. A parametric study of the influence of temperature, relative humidity, inlet pressure, and oxygen excess ratio on fuel cell performance is conducted based on this model. A set of PEM fuel cell-battery power system controllers are developed. The results show that the air supply control system can well deliver the sufficient reactants for fuel cell stack; the humidification control system is able to increase the fuel cell system performance by maintain the fuel cell stack relative humidity; the system power management system has the function of accurately distribute the demand power between fuel cell and battery as well as maintain the system components life and emergency shutdown. A physical PEM fuel cell-power system with embedded control system is built to validate the simulation results as well as system demonstration. Validation results show that the simulation results match the trend of experiment results.

6.2 RECOMMEDATIONS

We can see from the results in Chapter 5, there are some physical limitations of hardware which limits the PEM fuel cell-battery power system from a better performance. A high pressure blower or air pump is needed to prevent the fuel cell stack from air starvation when demand current goes high. In order to power the high pressure blower or

air pump, and to increase the output voltage to fit the DC/DC converter's working voltage range, a larger fuel cell stack with higher output voltage is recommended for further study.

Also we can see from the experiment results, the fuel cell output voltage response tends to be slower as the relative humidity goes low. A physical humidification system is needed to improve the fuel cell system performance.

REFERENCES

- [1] Ryan O'Hayre, Suk-Won Cha, Whitney Colella and, Fritz B. Prinz *Fuel Cell Fundamentals*, Wiley 2006, ISBN-0-471-74148-5.
- [2] J. Larmini, A. Dicks *Fuel Cell Systems Explained*, John Wiley, Sons, Let 2002.
- [3] U.S. Department of Energy, *Fuel Cell Handbook* 5th edition; 2000.
- [4] J.H. Lee and T.R. Lalk. Modeling fuel cell stack systems. *Journal of Power Sources*, 73:229–241, 1998..
- [5] S. Akella, N. Sivashankar, and S. Gopalswamy. Model-based systems analysis of a hybrid fuel cell vehicle configuration. *Proceedings of 2001 American Control Conference*, 2001.
- [6] J.C. Amphlett, R.M. Baumert, R.F. Mann, B.A. Peppley, P.R. Roberge, and A. Rodrigues. Parametric modelling of the performance of a 5-kW proton-exchange membrane fuel cell stack. *Journal of Power Sources*, 49:349–356, 1994.
- [7] D.D. Boettner, G. Paganelli, Y.G. Guezennec, G. Rizzoni, and M.J. Moran. Proton exchange membrane (PEM) fuel cell system model for automotive vehicle simulation and control. *Proceedings of 2001 ASME International Mechanical Engineering Congress and Exposition*, 2001.
- [8] J. Kim, S-M Lee, and S. Srinivasan. Modeling of proton exchange membrane fuel cell performance with an empirical equation. *Journal of the Electrochemical Society*, 142(8):2670–2674, 1995.
- [9] M. Ogburn, D.J. Nelson, K. Wipke, and T. Markel. Modeling and validation of a fuel cell hybrid vehicle. *SAE Paper 2000-01-1566*.
- [10] R. Andrew, X.G. Li, Mathematical modeling of proton exchange membrane fuel

cells, *J. Power Sources* 102 (2001) 82–96.

- [11] S.-H. Ge, B.-L. Yi, A mathematical model for PEMFC in different flow modes, *J. Power Sources* 124 (2003) 1–11.
- [12] X. Yu, B. Zhou, A. Sobiesiak, Water and thermal management for Ballard PEM fuel cell stack, *Journal of Power Sources* 147 (2005) 184–195
- [13] J.T. Pukrushpan, A.G. Stefanopoulou, H. Peng, *Control of Fuel Cell Power Systems, Principles, Modelling, Analysis and Feedback Design*, Springer Verlag, 2004, ISBN 1852338164.14.
- [14] L. Benini , A. Bogliolo , G.D. Micheli, A survey of design techniques for system-level dynamic power management, *IEEE Transactions on Very Large Scale Integration (VLSI) Systems*, v.8 n.3, p.299-316, June 2000
- [15] L. Benini , G. D. Micheli, *Dynamic Power Management: Design Techniques and CAD Tools*, Kluwer Academic Publishers, Norwell, MA, 1998
- [16] T. D. Burd, T. A. Pering, A. J. Stratakos, and R. W. Brodersen. 2000. A dynamic voltage scaled microprocessor system. *IEEE J. Solid-State Circ.* 35, 11 (Nov.), 1571–1580.
- [17] L. H. Chandrasena. and M. J. Liebelt, 2000. Energy minimization in dynamic supply voltage scaling systems using data dependent voltage level selection. In *Proceedings of the International Symposium on Circuits and Systems*, 525--528.
- [18] Y. Cho , N. Chang , C. Chakrabarti , S. Vrudhula, High-level power management of embedded systems with application-specific energy cost functions, *Proceedings of the 43rd annual conference on Design automation*, July 24-28, 2006, San Francisco, CA, USA

- [19]K. Choi , R. Soma , M. Pedram, Off-chip latency-driven dynamic voltage and frequency scaling for an MPEG decoding, Proceedings of the 41st annual conference on Design automation, June 07-11, 2004, San Diego, CA, USA
- [20]E. Chung , L. Benini , G. D. Micheli, Dynamic power management using adaptive learning tree, Proceedings of the 1999 IEEE/ACM international conference on Computer-aided design, p.274-279, November 07-11, 1999, San Jose, California, United States
- [21]L. Gao, Z. Jiang, and R. A. Dougal, 2005. Evaluation of active hybrid fuel cell/battery power sources. IEEE Trans. Aerospace Electron. Syst. 41, 1 (Jan.), 346--355.
- [22]W. Gao, 2005. Performance comparison of a fuel cell-battery hybrid powertrain and a fuel cell-ultracapacitor hybrid powertrain. IEEE Trans. Vehic. Technol. 54, 3 (May), 846--855.
- [23]D. Gervasio, S. Tasic, and F. Zenhausern, 2005. A room temperature micro-hydrogen generator. J. Power Sources 149, 15--21.
- [24]M. J. Gielniak, and Z. J. Shen, 2004. Power management strategy based on game theory for fuel cell hybrid electric vehicles. In Proceedings of the Vehicular Technology Conference (VTC) 6, 4422--4426.
- [25]AMETEK 3.0 BLDC 12VDC Low-Voltage Blower Data Sheet, www.ametek.com.
- [26]Y. Cao, A Simulink model configurable to buck, boost and buck-boost DC-DC converters with PWM PI control, 2008, www.matlab.com.
- [27]O. Tremblay, L. A. Dessaint, A. I. Dekkiche, A Generic Battery Model for the

Dynamic Simulation of Hybrid Electric Vehicles, Vehicle Power and Propulsion Conference, 2007. VPPC 2007. IEEE 9-12 Sept. 2007, pp. 284-289.

[28]K. Kato, A. Negishi, K. Nozaki, I. Tsuda, K. Takano, PSOC cycle testing method for lithium-ion secondary battery. *Journal of Power Sources* 117, no. 12 (2003): 118-123.

[29]Y. Wang and C.Y. Wang, Transient Analysis of Polymer Electrolyte Fuel Cells, *Electrochimica Acta*, 50, (2005) 1307-1315.

[30]Y. Wang and C.Y. Wang, Dynamics of Polymer Electrolyte Fuel Cells Undergoing Load Changes, *Electrochimica Acta*, 51 (2006) 3924- 3933.

VITA AUCTORIS

Yan Zhang, born on July 2nd, 1985 in the city of Hohhot, Inner Mongolia, China. Finished high school in No.2 middle school of Hohhot. Undergraduate studied in Inner Mongolia University of Technology majoring Automation during 2004-2008. Received a bachelor degree of engineering. Studied during 2008-2010 in University of Windsor, Ontario, Canada for a Master of Applied Science in Mechanical Engineering.